Optimizing Lane Changing Safety: Development and Evaluation of Intelligent Decision-Making Algorithms

Charles Diwivedi Parakesh

A Thesis Submitted to

The department of Mechanical Engineering

School of Mechanical, Chemical, and Materials Engineering

Presented in Partial Fulfillment of the Requirement for the degree of Master's in Automotive Engineering

Office of Graduate Studies

Adama Science and Technology University

June, 2023

Adama, Ethiopia

Optimizing Lane Changing Safety: Development and Evaluation of Intelligent Decision-Making Algorithms

Charles Diwivedi Parakesh

Advisor: Dr. Getachew Alemayew

A Thesis Submitted to

The department of Mechanical Engineering

School of Mechanical, Chemical, and Materials Engineering

Presented in Partial Fulfillment of the Requirement for the degree of Master's in Automotive Engineering

Office of Graduate Studies

Adama Science and Technology University

June, 2023

Adama, Ethiopia

DECLARATION

I hereby declare that this Master Thesis entitled “**Optimizing Lane Changing Safety: Development and Evaluation of Intelligent Decision-Making Algorithms”** is my original work. That is, it has not been submitted for the award of any academic degree, diploma or certificate in any other university. All sources of materials that are used for this thesis have been duly acknowledged through citation.

______________________________	________________	_________________
Name of student	Signature	Date

RECOMMENDATION

I, the advisor of this thesis, hereby certify that I have read the revised version of the thesis entitled "**Optimizing Lane Changing Safety: Development and Evaluation of Intelligent Decision-Making Algorithms**" prepared under my guidance by Charles Diwivedi Parakesh submitted in partial fulfillment of the requirements for the degree of Master's of Science in Automotive Engineering. Therefore, I recommend the submission of the revised version of the thesis to the department following the applicable procedures.

Major Advisor/Supervisor	Signature	Date

APPROVAL

I, the advisor of the thesis entitled "**Optimizing Lane Changing Safety: Development and Evaluation of Intelligent Decision-Making Algorithms**" and developed by Charles Diwivedi Parakesh, hereby certify that the recommendation and suggestions made by the board of examiners are appropriately incorporated into the final version of the thesis.

Major Advisor	Signature	Date

We, the undersigned, members of the Board of Examiners of the thesis by Charles Diwivedi Parakesh have read and evaluated the thesis entitled "**Optimizing Lane Changing Safety: Development and Evaluation of Intelligent Decision-Making Algorithms**" and examined the candidate during open defense. This is, therefore, to certify that the thesis is accepted for partial fulfillment of the requirement of the degree of Master of Science in Automotive Engineering.

Chairperson	Signature	Date
Internal Examiner	Signature	Date
External Examiner	Signature	Date

Final approval and acceptance of the thesis is contingent upon submission of its final copy to the Office of Postgraduate Studies (OPGS) through the Department Graduate Council (DGC) and School Graduate Committee (SGC).

Department head	Signature	Date
School Dean	Signature	Date
Office of Postgraduate Studies, Dean	Signature	Date

ACKNOWLEDGEMENT

I would like to extend my heartfelt appreciation to the Divine Creator for His gracious support thoughout the completion of this thesis. I am immensely grateful to my advisor, Dr. Getachew Alemayew, whose unwavering dedication, guidance and insightful advice have beet instrumental in overcoming various challenges encountered during the course of this research. I would also like to acknowledge the invaluable mentorship provided by Dr. Ramesh Babu Nallamothu, who has been akin to father figure, offering both technical expertise and motivational encouragement. My brother, Mr. Dawit Berhanu, deserves special recognition for his unwavering encouragement and unwavering financial and material support. I must express my deepest gratitude to my friend, Dr. Yisak Tola, who not only shared his extensive knowledge of both the theoretical foundations and software applications but also pushed me to persevere until the very end. Furthermore, I would like to extend my thanks to my family, friends, the staff of ASTU, and all other individuals and organizations who have played a significant role in the progress of this final thesis. Last but certainly not least, I am indebted to the creators of MATLAB and CarSim, whose exceptional products have been the cornerstone in transforming diligent effort into fruitful outcomes.

TABLE OF CONTENTS

CONTENT PAGE

LIST OF TABLES

LIST OF FIGURES

List Of Acronyms and Abbreviations

ACC	Adaptive Cruise Control
ADAS	Advanced Driving Assistance System
AEM	Autonomous Emergency Maneuvering
AV	Autonomous Vehicle
CACC	Cooperative Adaptive Cruise Control
CA	Collision Avoidance
CPU	Central Processing Unit
CW	Collision Warning
ESC	Electronic Stability Control
LKAS	Lane Keeping Assistance System
LC	Lane Change
LK	Lane Keeping
LKC	Lane Keeping Control
MPC	Model Predictive Control
NHTSA	National Highway Traffic Safety Administration
TLC	Time to Lane Crossing
TTC	Time to Collision

Abstract

Statistics show that driver irresponsibility is mostly to blame for accidents, particularly when a driver is about to change lanes or pass another car, which increases the likelihood of an accident. Furthermore, because overtaking involves both dynamic and complex functions as well as the challenging task of implementing control strategies and electronic control systems, like steering, throttle, and brake control, it is one of the most challenging and complex functions for the development of autonomous driving technologies. In this thesis, a safe overtaking technique for an autonomous vehicle is shown, based on model predictive control and vehicle dynamics. A sensors-based lane-detection system is used to estimate TLC (Time to Lane Crossing) so that a timely and accurate choice may be made regarding whether to overtake or stay in the lane. Overtaking is one of the trickiest maneuvers that requires both lane keeping and lane shifting. Next, maintain the smallest possible safe distance while selecting the optimal vehicle controller, such as throttle, brake, and steering angle. It can concurrently guarantee the maintenance of steering velocity and longitudinal acceleration to protect drivers. In this manner, the study involves the integration of AEM (Autonomous Emergency Maneuvering), LKAS (Lane Keeping Assistance System), and ACC (adaptive cruise control) to have more accurate and realistic lane changing, lane departure/merging, and overtaking processes. The vehicle modes is imported from Carsim to be analyzed the dynamics and kinematics on Simulink. Later on, the system is validated by CarSim/Simulink software combined by Matlab. The simulations showed how adaptable the suggested overtaking judgment and control approach was under different driving conditions. The simulation result outcome the desired the vehicle decision action with respect to the scenarios stated with interaction with the actor vehicles and the road condition.

Keywords: Overtaking, lane departure/merging, Autonomous emergency maneuvering (AEM), lane keeping assistance system (LKAS), adaptive cruise control (ACC)

CHAPTER ONE

INTRODUCTION

1.1. Background

Every year, traffic accidents result in the deaths of millions of individuals (Ivars, 2007). By creating passive safety devices like seat belts, air bags, and collision zones, researchers attempted to solve this catastrophic dilemma (Report et al.). Even though these passive controls were very helpful, there must be other ways to keep accidents at manageable levels. Through improvements in proactive and active safety systems, this objective is getting closer to realization (Ararat & Güvenç, n.d.).

The car industry has shifted to Advanced Driving Assistance Systems (ADAS) despite the fact that research on these topics began with Autonomous Highway Systems (AHS), given the fact that advancements on AHS can only be realized over the long term (Basztura, 2003).

Economic factors are also a major factor in the high interest in ADAS. (Vahidi & Eskandarian, 2003) Driving assistance systems improve traffic efficiency and lower fuel use. According to Jula et al. (2000), highway capacity is influenced by both vehicle speed and inter-vehicle spacing. With increasingly intelligent vehicles, it will be feasible to safely actualize rapid vehicles following each other in close quarters, increasing the capacity of the route. Low velocity changes and vehicle communication capabilities, on the other hand, will reduce fuel usage (Vahidi & Eskandarian, 2003).

The ADAS, which includes systems like lane keeping, lane departure prevention, driver condition monitoring, night vision, adaptive cruise control, and stop and go assistants, includes collision warning (CW) and collision avoidance (CA) systems as a significant component.

According to (Lin et al., 2021), the market share of autonomous vehicles has grown over time. Although the COVID-19 pandemic-induced economic downturn caused the market to shrink by around 3% in 2020, the market is predicted to rise by about 60% from 2021 to 2023 (Martin Placek, 2021). Nearly 60% of all new automobiles in 2030 will have Level 2 autonomy, and these vehicles are anticipated to rule the market. Additionally, level 3 and level 4 technologies will be standard on about 8% of all new vehicles. A genuinely driverless vehicle does not yet exist, despite the efforts of numerous research groups, automakers, and top institutions in the field of autonomous vehicle technology. Reliability is one of the biggest problems. Autonomous technologies, such as environment sensing, control, and decision-making, still have a lot of practical challenges to overcome, especially in challenging traffic circumstances, tasks, or bad weather.

Statistics from the Highway Traffic Safety Administration and the Department of Transportation (NHTSA, 2021) show that in the first nine months of 2020, 28,190 people lost their lives in car accidents. Nearly 94% of fatal collisions were linked to driver error, including inattentiveness, panic, inexperience, and slow reaction times, particularly when drivers planned to make lane changes or pass another car, which were the most frequent reasons for collisions.(Lin et al., 2021) In addition, a number of studies (Clarke et al., 1998) have highlighted how a lack of skills, roadway capacity, and information processing abilities during an overtaking operation result in deadly auto accidents. The failure of a motorist to recognize risks during lateral maneuvers accounts for over 75% of all traffic accidents. In order to eliminate human mistakes, automated overtaking systems must be developed and put into use. These systems have the potential to save lives and effectively reduce accidents. Because of the dynamic and challenging tasks involved in steering and speed control, overtaking is one of the most challenging and complex operations for the implementation of automated driving technologies. Automation of the overtaking maneuver necessitates high-precision environment perception technology to keep track of the surrounding traffic conditions as well as the ability to foresee probable instances of time-sensitive decision-making and action implementation. Lane keeping, lane changing, and overtaking are complicated driving operations that autonomous or semi-autonomous cars must be capable of doing. These actions are necessary in everyday driving circumstances and can improve traffic efficiency, particularly on one- and two-lane roads.

1.2. Statement Of the Problem

On the road, the drivers of the vehicles must frequently change lanes. Crashes and accidents may happen as a result of the motorist making poor decisions in unforeseen and challenging circumstances. (Eskandarian, 2012) Run-off-road crashes account for 34% of traffic deaths. Side-swipe incidents can also happen as a result of unintended or poorly timed lane departures. Numerous strategies have been developed to reduce these incidents. This is the reason why vehicles today come equipped with lateral control and warning systems. To lessen collisions brought on by these conditions, autonomous systems must be deployed. Therefore, autonomous vehicles have a wide range of driver assistance and collision prevention systems. In terms of effectiveness and other aspects, such lane departure, more work needs to be done.

Due to the necessity of overtaking and passing barriers, there are numerous potential outcomes during lane departures. These situations call for split-second judgements that are accurate and rapid. Therefore, studies that take into account varied lane departure conditions in depth, as this paper suggests, are needed. This thesis deals with issues caused by unobserved overtaking scenarios and the application of cutting-edge systems that address challenges in the application of collision avoidance, notably in lane changing. The design of a collision avoidance system combining several technologies and research is required to produce safer and more accurate lane departure circumstances. This encompasses the notions of vehicle dynamics, throttling, Adaptive Cruise Control (ACC), Electronic Power Steering (EPS), Autonomous Emergency Maneuvering (AEM), and Advanced Driver Assisting System (ADAS). The deployment of multiple sensors is also recommended to maintain decision correctness.

1.3. Objectives Of the Study

1.3.1. General Objective

The general objective of this thesis work is to reduce the potential vehicle collision arising from lane departure by applying an active collision avoidance system through collision prediction approach, emergency maneuvering, braking, and throttling.

1.3.2. Specific Objectives

The specific objectives are as follows:

- Developing the vehicle dynamics model considering the vehicle speed variation lane changing/merging safety distance by CarSim.
- Integration of sensors, controller and actuators in Matlab-Simulink.
- Developing Adaptive Cruise control which is precise and sustainable for most complex driving conditions.
- Employing predictive control to derive an optimal vehicle controller, such as throttle, brake, and steering angle control through CarSim-Simulink platform.
- Conducting CarSim simulations to validate the control performance in the proposed cooperative driving strategy.

1.4. Significance Of the Study

- The advancement of intelligent decision-making algorithm is crucial to overcome sophisticated scenarios which is safer and more reliable in contrast with previous studies.
- The algorithm is expected to bring accurate actions given the sample of obstacle scenarios which are road scenarios and the actor vehicles.
- The advancement of semi-automated vehicles involving LKAS and ACC minimized collusions and damages.
- Formulation of predictive control system in active collision avoidance system provides the safety prior to the accident.
- Decision-making strategies that is able to implement in Autonomous vehicles equipped with electronic power steering, brake and throttle eases the driver’s stress and burden.
- The most important characteristics associated with motion control and decision-making strategies are identified.
- A framework that combines vehicle dynamics, active safety system, and ACC results the advancement in the autonomous system of automotive industries.

1.5. Delimitations and Limitations of the Study

Three levels of analysis are done to determine how automation in vehicles affects safety. The "vehicle" level, which is the initial level, emphasizes the advantages of AVs in minimizing or doing away with driver-related errors. The "transportation" level, which is the second level, examines how AVs can lessen traffic congestion and collisions. The "society" level, which focuses on improvements in car crashes and public health, is the third level. This thesis makes a direct or indirect contribution to each of the three stages of automation in terms of safety. This thesis has a positive effect on AV safety at the level of the vehicle by conducting research on the subject and recommending strategies and algorithms meant to improve traffic safety by conducting research on the subject and recommending strategies and algorithms meant to improve traffic safety. On the transportation level, the positive impact is achieved by addressing AVs’ safety and performance in mixed-traffic scenarios, and on the society level by developing a framework that aims at reducing injury severity for occupants of vehicles.

This thesis has mostly focused on vehicle dynamics and predictive control in situations where collision is preventable in terms of AV research and development domains. However, this thesis does not address the actions of vulnerable road users like bicycles and pedestrians. Additionally, the degree of the post-collision damage to the car and the property is not taken into account. This is because preventing accidents is prioritized over minimizing their effects. This study is only concerned with the decision-making process in lane-changing occurrences, but it can be applied to other circumstances when collision avoidance is required. Given that it is discovered that lane departure is the most complex and collision-prone circumstance when operating a vehicle, a specific study in this area is provided.

CHAPTER TWO

LITERATURE REVIEW

2.1. Introduction

Both safety and highway capacity are impacted by the headway or distance between vehicles. The separation must be sufficient to ensure no collisions throughout all feasible vehicle moves in order to provide collision-free vehicle following. Various forms of vehicle crashes, including rear-end collisions, single vehicle road departure accidents, side-wipe collisions, and angle collisions, are included in lane changing/merging accidents. In 1991, lane changing/merging collisions made up around 4.0% of all crashes that the police documented, and they caused about 0.5% of all fatalities.(J.-S.Wang & R. R. Knipling, 1994)

Although the problem of lane change crashes is minor in comparison to other crash types and does not contribute significantly to traffic fatalities, this crash type is accountable for 10% of all crash-related traffic delays, which frequently generate congestion. Travel time is lengthened by traffic delays and congestion, which also have a detrimental economic effect (J. D. Chovan et al, 1994). In reality, altering relative velocities and widening the longitudinal space between vehicles can lessen the likelihood of merging collisions. Given that vehicle speed and longitudinal inter-vehicle spacing are inversely correlated with roadway capacity, a significant decrease in speed or significant increase in spacing results in a low-capacity highway system. The headway setting for a high-capacity roadway system should be as small as possible. The setting of minimum safety spacing (MSS) between vehicles for a collision-free environment is crucial from a safety and capacity point of view because safety cannot be cheaply sold off. The issue of avoiding obstacles was studied. (Godbole et al., 1997) and (Z. Shiller & S. Sunder, 1998) thought about the issue of a collision between a moving vehicle and an already-existing static obstruction, such a broken-down car or a big object. Two options were evaluated for avoiding the obstruction: halting in the same lane or making a lane change.(Z. Shiller & S. Sunder, 1998) created curves that define the clearance and stopping for the collision avoidance maneuver. The phase-plane, which plots the starting longitudinal velocity of the vehicle under consideration against its distance from the obstacle plane, is divided into three sections by these curves. The vehicle executes a routine (non-emergency) full stop or routine lane-changing action in Region I. Only the standard lane-changing maneuver is performed by the vehicle in Region II, whereas the full stop maneuver is performed by the vehicle in Region III while still in the same lane. If possible, lane change takes precedence over a full stop when a vehicle is in Region I. When a collision is about to happen, the car is in Region III. In that situation, it is demonstrated that a sudden stop in the same lane lessen the severity of the crash and is thus preferable to lane switching. The lane changing maneuver for obstacle avoidance problem was conceptualized by (Godbole et al., 1997) as an optimal control problem. The collision avoidance problem is presented as an optimization problem for routine lane changes, where the goal is to reduce the time required to complete the maneuver by choosing the proper lateral and longitudinal control inputs. The lateral and longitudinal control inputs are computed to reduce the longitudinal distance between the vehicle and the obstruction in an emergency lane-changing situation. Both of the aforementioned works (Godbole et al., 1997) and (Z. Shiller & S. Sunder, 1998) do not consider the cars in the lanes next to you, which might be a hindrance to lane switching.

(Bascunana & Mesa, 1997) established the parameters for both safe and unsafe lane switching. For the two vehicles engaged in the lane-changing action, the conditions were achieved. Vehicle 1 executes a merging maneuver to the opposite lane when the cars are initially traveling in two adjacent lanes as shown in figure 2. He took into account the following four situations:

Case I: Vehicle 1 wishes to complete the lane change with constant longitudinal velocity but its beginning longitudinal velocity is lower than that of vehicle 2, thus it follows vehicle 2;

Case II: Vehicle 1 plans to complete the journey by continuously applying longitudinal acceleration even though its beginning longitudinal velocity is lower than that of vehicle 2;

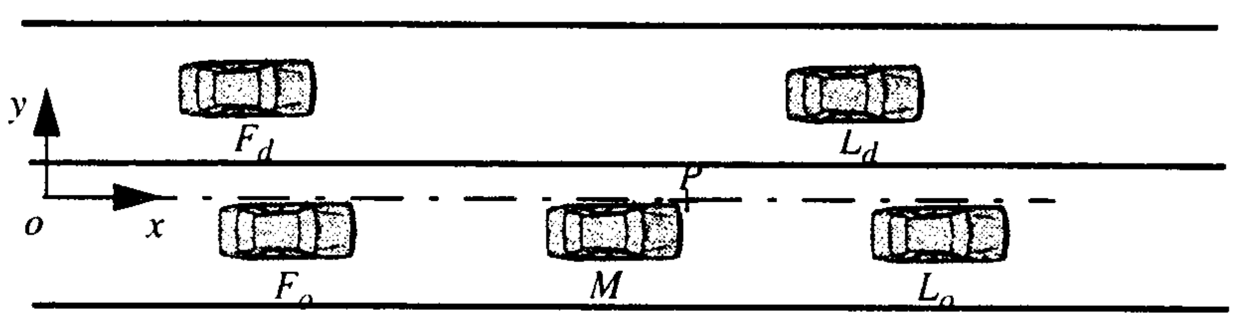

Figure 1. Pre-lane changing configuration showing position of merging vehicle “M” (Bascunana & Mesa, 1997)

Case III: In this scenario, vehicle 1 has a higher initial longitudinal velocity than vehicle 2, and it intends to complete the lane change with constant longitudinal velocity while leading vehicle 2.

Case IV: In this scenario, vehicle 1 has a higher initial longitudinal velocity than vehicle 2, and it intends to complete the lane change with constant longitudinal deceleration while trailing vehicle 2.

The issue of safe lane switching and merging maneuvers on highway systems is looked at in the paper. A general approach to determine if a specific lane change or merging maneuver is safe, or collision-free, is offered by examining the kinematics of the vehicles engaged in the scenario. An all-encompassing algorithm for determining the minimal longitudinal safety spacing, or MSS, for each engaged vehicle, is outlined. In other words, given a specific lane change/merging scenario, the smallest longitudinal spacings that the vehicles involved in the lane changing action must initially maintain to avoid colliding is determined.

(Malayjerdi et al., 2022) studied on self-driving cars, particularly autonomous minibuses, sometimes known as autonomous shuttles, are nearing commercialization inseverable places throughout the world. Most autonomous shuttle initiatives, however, are still in the testing phase and can only demonstrate a small number of autonomous functionalities. One fundamental maneuver is to switch lanes to avoid crashes, like those with parked cars. The majority of the commercially available automation level 4 autonomous shuttles have trouble doing this task, even though it may seem straightforward to humans. Vehicle safety, accident rates, and environmental effect are all things that research and manufacturers are working to improve. With basic path planning algorithms, the first generation of autonomous shuttles could only operate in structured environments. The self-driving algorithm must be able to enable more complicated operations like lane changes, overtaking, etc. because new self-driving cars in automation levels 4 and 5 are anticipated to drive similarly to human drivers.

(Hegeman et al., 2005) Up to 10% of driving accidents are allegedly caused by lane change incidents. It is obvious that the lane change is a dangerous maneuver even for human drivers, and autonomous shuttles will have a very difficult time lane changing to perform a safe overtaking. Overtaking algorithms need in-depth knowledge of the surroundings in all directions as well as intricate calculations of the static and moving items in the scene (González et al., 1999).The planning algorithm also needs knowledge of additional issue aspects, such as diverse weather conditions, various traffic circumstances, interaction with other road users (cars and pedestrians), and various road quality (C. Li et al., 2016). Path planning is therefore seen as a crucial component of the software for automated shuttles (Carroll et al., 1992). Depending on the planning scope, it is often separated into global and local path planners. Global planners focus on creating a path that reduces travel time and distance by taking into account the complete environment from the start point to the target point. In contrast to global route planners, local path planners put more emphasis on enhancing driving safety by utilizing sensory data and information on the stability of the vehicle during the obstacle avoidance phase.

Theoretical Background

Architecture of the Collision Avoidance System.

(Wu et al., 2020) examined the collision-avoiding algorithm's general structure, which is depicted in Figure 1. A danger monitor, an autonomous steering controller, and a differential brake controller make up the structure. The risk monitor is made to employ the relevant risk metrics in relation to the time to collision (TTC), the braking threat number (BTN), and the steering threat number (STN). In addition, the metrics are used to determine whether a lateral control intervention Is required.

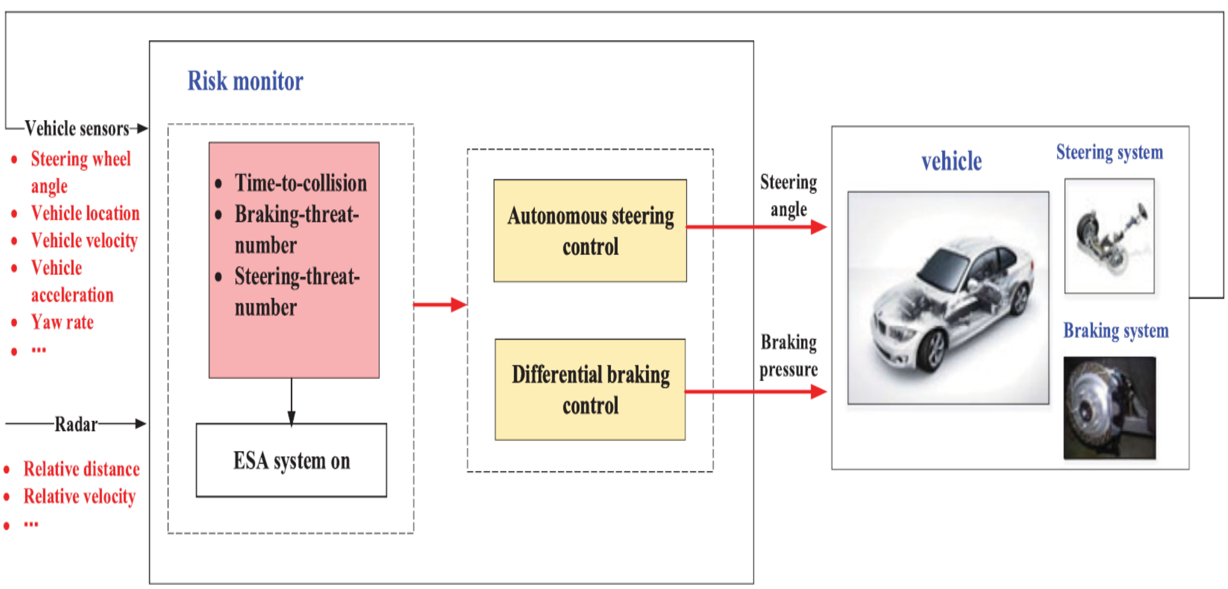

Figure 2: The overall structure of the collision-avoiding algorithm (Wu et al., 2020)

The AES system is turned on if an emergency steering intervention is necessary. The autonomous steering algorithm consists of two components according to the process of collision avoidance, which is divided into two stages, rather than sharing with the driver for collision avoidance. The feedforward controller based on nonlinear handling dynamics is used in the first stage to prevent a collision by applying a constant lateral acceleration. The MPC-based controller, which can better handle restrictions, is designed in the second stage to steer the subject vehicle along the centerline of the adjacent lane once it is out of danger of colliding. Due to the impact on the vehicle dynamics, there is a greater need for vehicle stabilization when the emergency steering maneuver is used while traveling on the highway. To enhance the vehicle steadiness, we developed the differential braking algorithm. The differential braking controller is built as a compensator to balance the demands of vehicle stability and collision avoidance, as opposed to tracking the target yaw rate computed by solely taking into account the vehicle stabilization or path tracking. Finally, a hardware-in-the-loop (HIL) platform experiment was run to confirm the suggested emergency collision avoidance strategy's real-time performance and efficiency.

2.2. Existing Decision-Making Algorithm for Collision Avoidance System

(M. Li et al., 2019) designed the system's general structural design, which is depicted in Figure 3, for the vehicle's lane change overtaking anti-collision system.

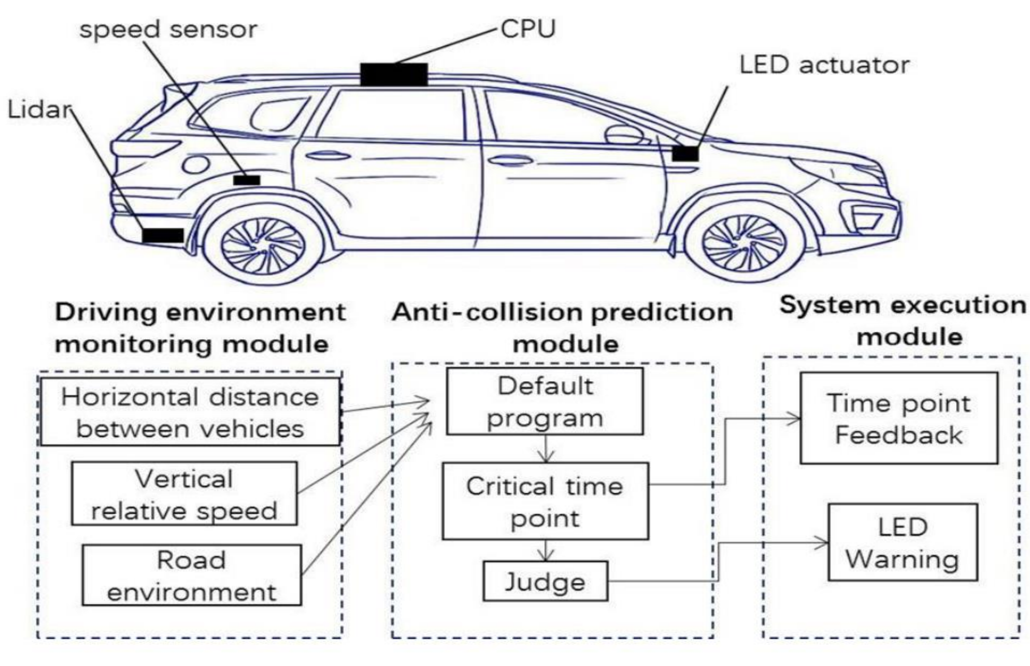

Figure 3: Overall structural design of the vehicle lane change overtaking anti-collision system(M. Li et al., 2019)

The driving environment monitoring module, the anti-collision prediction module, and the system execution module are the three modules that make up the system, as can be seen in Figure 2. The driving environment monitoring module uses the laser radar and speed sensor to gather data from the road environment, such as the lateral distance between the vehicle and the longitudinal relative speed, and sends it to the anti-collision prediction module's central processor. The AT89C51 single-chip microcomputer processes the anti-collision prediction module's central processing unit, which is its main component. The processing operation is carried out by the preset program after the driving environment monitoring module's data has been obtained. The critical lane change time point is then calculated, and the current lane change time is assessed to see if it is reasonable based on the trajectory route and steering wheel angle of the vehicle. Two components make up the system's execution module: a feedback display unit and an LED warning light. The CPU will determine the key overtaking time point and then communicate it to the driver via the feedback display unit. It will then determine whether the present driver's driving behavior is appropriate for a lane change and an overtake. The system can prevent collisions and protect the driver if it doesn't turn on the LED and send out an alarm to alert the driver via the execution module.

(Lin et al., 2021) The suggested autonomous overtaking system is implemented using an electric golf car, and Figure 4 depicts the test vehicle's system configuration.

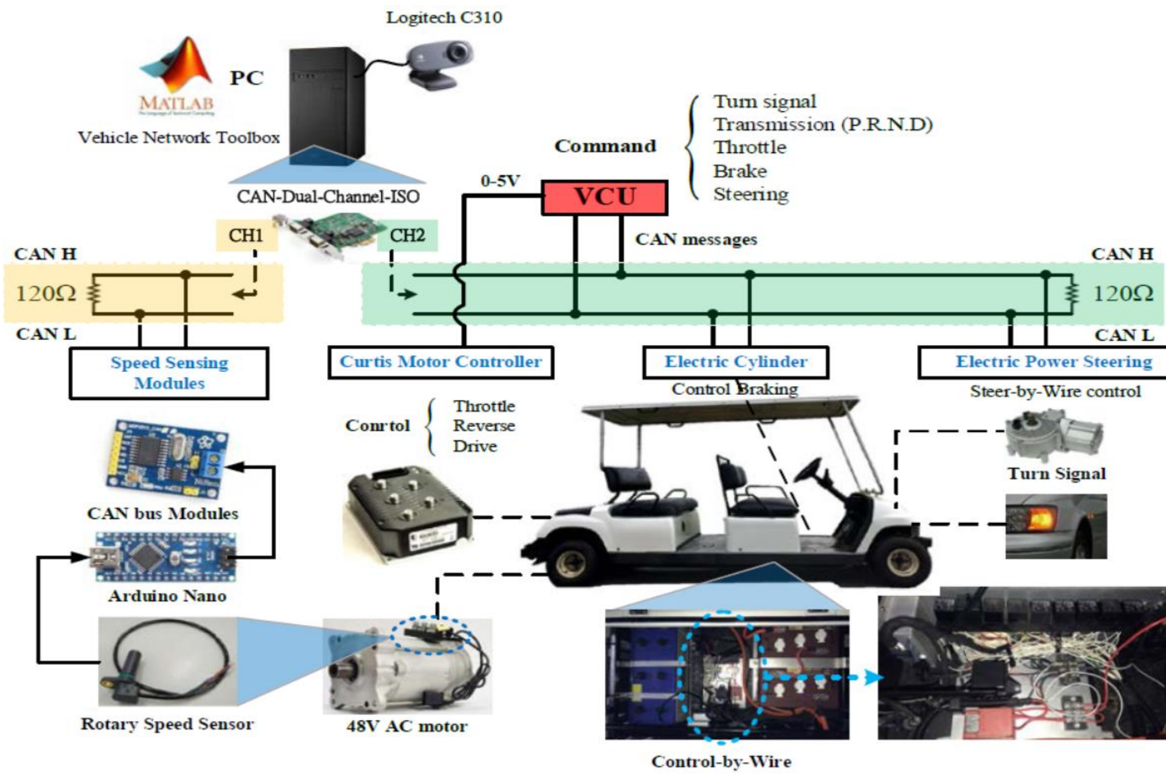

Figure 4: Vehicle configuration for implementation of the proposed autonomous overtaking system(Lin et al., 2021).

The three functional modules that make up the investigated autonomous overtaking system are perception, overtaking decision-making, and vehicle control. Figure 5 depicts the suggested autonomous overtaking system's architecture. Environment perception, which depends on the lane lines, comes before vehicle detection via eye observation in the upper processing steps. Perception tells us how far a moving object is from us, where other cars are in relation to us, and where the lane lines are.

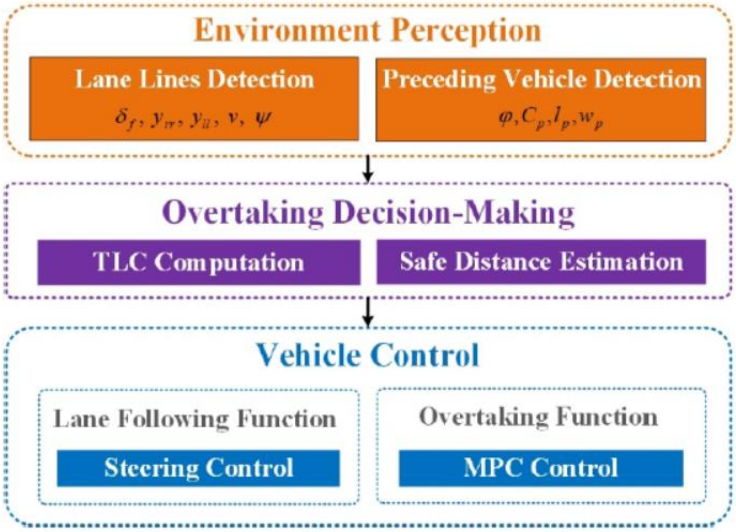

Figure 5: The architecture of the proposed autonomous overtaking system (Lin et al., 2021).

According to research by (Chiang et al., 2014), a proposed system that can enable automatic driving with a variety of driving behaviors is developed as a hierarchical architecture with two layers (Fig. 6). A decoupled longitudinal and lateral control can be utilized to steer the vehicle through various driving maneuvers without pushing the physical boundaries of the vehicle. Additionally, the driver employs a switching method based on basic control laws rather than sophisticated nonlinear control laws after witnessing human drivers in action. As models of the driver's behavior involved in situational evaluation (the data fusion stage) and physical abilities (the automation stage), respectively, this switching mechanism and the auxiliary control rules can be used.

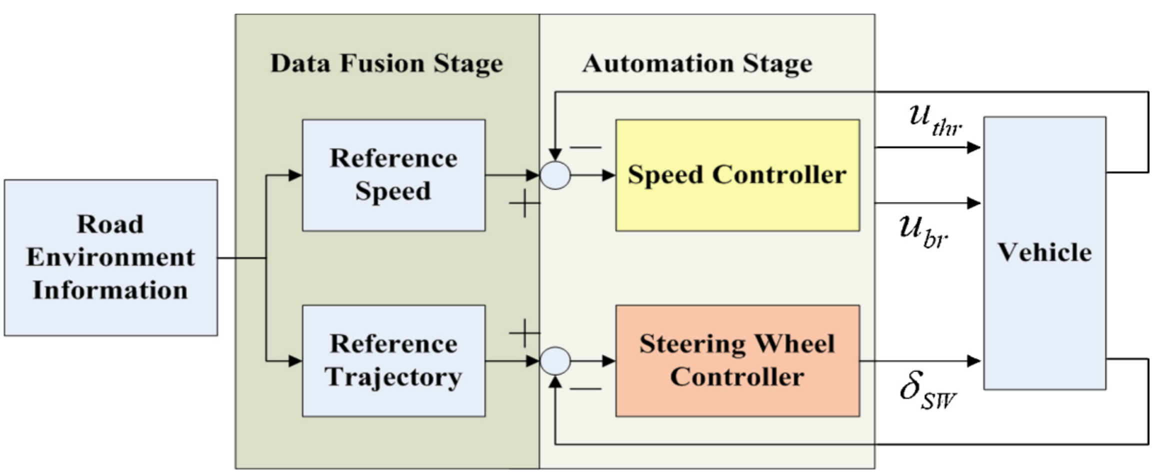

Figure 6: Structure of controller/vehicle system (Chiang et al., 2014)

In the research of (Karunakaran et al., 2022) the cut-in and cut-out lane change scenario types—which are illustrated in figure 6—are of special interest. A cut-in is considered to occur when a challenging vehicle enters the ego-vehicle lane (figure 7a). A cut-out scenario, on the other hand, takes place when the front challenging vehicle switches from the ego-vehicle's lane to a nearby one (figure 7b).

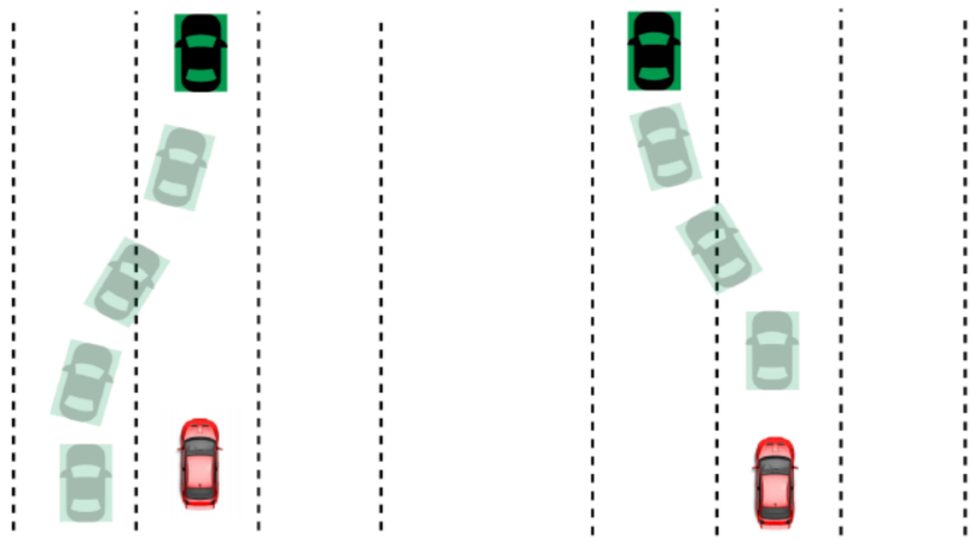

(a) Cut-in scenario: the challenging vehicle changes the lane to ego vehicle's lane.

(b) Cut-out scenario: the challenging vehicle changes the lane from ego vehicle's lane.

Figure 7: Lane change scenario types, where the ego vehicle is in red, challenging vehicle is in green. (Karunakaran et al., 2022)

Paper used the scenario extraction framework from our previous work to capture the parameters proposed in this paper. The data used in this paper to model real-world scenarios was collected using Volkswagen Passat station wagon that is mounted with IBEO and SICK lidars. The placement of the lidars on the vehicle is shown in the Figure 6. The on-board computer processes the sensor data to detect and track the objects up to 200 meters.

2.3. Rear-End Collision Avoidance Systems

The algorithms of rear-end collision avoidance systems are based on the likelihood of a rear-end collision by calculating the critical distances between two vehicles following one another and comparing this with the current inter-vehicle separation to apply the appropriate actions for various scenarios(Ararat & Güvenç, n.d.). Figure 8 illustrates the fundamental geometry of a rear-end collision, where V denotes velocity, a denotes deceleration, and d is the separation between the two vehicles.

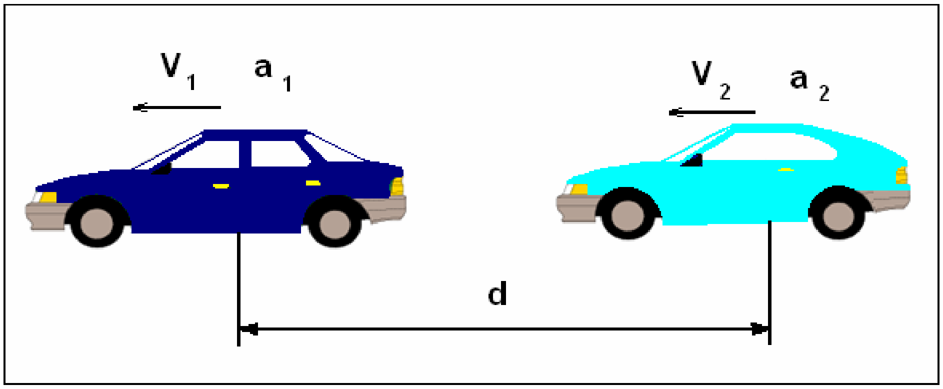

Figure 8 **:** Basic Geometry of Rear End Collision(Ararat & Güvenç, n.d.)

The Mazda Algorithm

The critical braking distance is determined by this system using an algorithm based on kinematical analysis. The computed distance must be regarded as a critical warning distance because it is too conservative for braking. The formula for the crucial warning distance d_w is

$$d_w = \frac{1}{2}\left(\frac{v^2}{\alpha_1} - \frac{(v - v_{rel})^2}{\alpha_2}\right) + V\tau_1 + V_{rel}\tau_2 + d_0 \qquad (2.1)$$

where d_0 represents the headway offset, v represents the speed of the car in front of it, V_{rel} represents the relative speed between the two, $\tau_1$represents the system delay, τ_2 represents the driver delay, and 1 and 2 represent the maximum decelerations of the two vehicles, respectively. This method assumes that after a driver delay of two seconds and a system delay of one second, the leading car starts to brake with a maximum deceleration of two and the following vehicle starts to brake with a maximum deceleration of one. The crucial warning distance is given a headway offset of d_0 to increase the algorithm's conservatism (Doi et al., 1994).

The Honda Algorithm

Honda's system is founded on data from experiments. The formula for the critical warning distance d_w is

$$d_w = 2.2V_{rel} + 6.2 \qquad (2.2)$$

Where V_{rel} is the difference in velocity between the vehicles in front and behind. Equation (2.2) is used to calculate the crucial warning distance, which is less than the typical maneuver distance for collision avoidance. Collision experiments with various drivers are used to get the average distance (Fujita et al., 1995).

The PATH Algorithm

The PATH algorithm is a modified version of Mazda's algorithm (Doi et al., 1994). The critical warning distance d_w is given by

$$d_w = \frac{1}{2}\left(\frac{v^2}{\alpha} - \frac{(v-v_{rel})^2}{a}\right)+v\tau+d_0 \qquad (2.3)$$

where d_0 is the headway offset, v is the velocity of the following vehicle, V_{rel} is the relative velocity between following and leading vehicle, α is the maximum deceleration of the vehicles and τ is the total delay for the system and driver.

The PATH algorithm aims to obtain a more conservative warning distance than Mazda. However, warning is scaled by a non-dimensional warning value *w* given by

$$w=\frac{d-d_{br}}{d_w-d_{br}} \qquad (2.4)$$

where d is the present distance and d_{br} is the critical braking distance which is calculated as

$$d_{br} = v_{rel}\tau \frac{1}{2}\alpha\tau^2 \qquad (2.5)$$

Braking distance shows the distance where there is nothing to do even driver notices the collision risk. This distance is simply calculated by kinematical formulation used for calculating traveled road with initial velocity and constant deceleration rate. Total time which is used in formulation equals to total delay that is sum of driver and system delays. Figure 9 shows d, d_w and d_{br} in schematic representation.

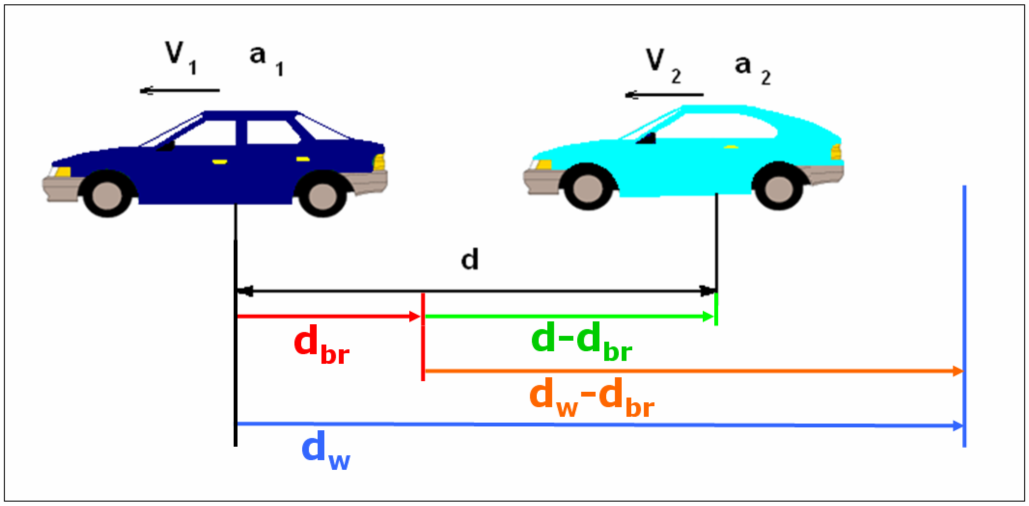

Figure 9: Schematic Representation of d, d_w and d_{br} (Doi et al., 1994)

This non-dimensional w value is used for grading warnings that are given to the driver.

Decreasing w shows increasing collision risk. w>1 means safe driving situation. Warning is given to the driver when w takes value between 0 and 1. PATH uses graduated Light Display to grade warnings with obtained w value. Graduated Light Display Screen shows colored signals changing between green to red where green shows safe driving and red shows last warnings to the collision. When w starts to decrease from 1 to 0, Graduated Light Display turns to yellow and finally red respectively from green gradually. The system applies the brake if w<0 (Seiler et al., 1998).

The NHTSA Algorithm

Kinematic analysis is also the foundation of the NHTSA algorithm. Along with velocity information, the NHTSA system also incorporates acceleration data. The method used to determine the crucial warning distance is

$$d_{w1}=0.1v+d_0-\frac{1}{2}(a-a_{max})(T_R)^2+\frac{1}{2}(a-a_{rel})(T_{LS})^2+(a-a_{max})T_RT_{FS}-V_{rel}T_{FS}-(a-a_{rel})T_{FS}T_{ls}+\frac{1}{2}a_{max}(T_{FS})^2 \quad (2.6)$$

$$d_{w2}=0.1v+d_0-V_{rel}T_M-\frac{1}{2}(a-a_{rel}-a_{max})(T_M)^2+(a-a_{max})T_MT_R-\frac{1}{2}(a-a_{max})(T_R)^2 \quad (2.7)$$

where d_0 is the headway offset, v is the velocity of following vehicle, V_{rel} is the relative velocity between following and leading vehicles, α is the acceleration of the following vehicle, α_{max} is the maximum deceleration of following vehicle, α_{rel} is the relative acceleration between following and leading vehicles, T_R is the reaction time, T_M is the time for the relative velocity between the two vehicles to reach zero and T_{LS} and T_{FS} are the stopping times of the leading and following vehicles, respectively. T_{LS}, T_{FS} and T_M are calculated by the following formulas.

where d_0 is the headway offset, v is the following vehicle's velocity, V_{rel} is the relative velocity between following and leading vehicles, is the following vehicle's acceleration, max is the following vehicle's maximum deceleration, α_{rel} is the relative acceleration between following and leading vehicles, T_R is the reaction time, T_M is the period of time it takes for the relative velocity between the two vehicles to reach zero, and T_{LS} and T_{FS} are the leading vehicle's stopping times These formulas are used to calculate T_{LS}, T_{FS}, and T_M.

$$T_{LS}= -\left(\frac{V-V_{rel}}{a-a_{rel}}\right) \tag{2.8}$$

$$T_{FS}=T_R- \frac{(V+aTR)}{a_{max}} \tag{2.9}$$

$$T_M= \frac{(v_{rel}-a_{rel}T_R)}{(a_{max}-a+a_{rel})} +T_R \tag{2.10}$$

Based on the values of T_{LS} and T_{FS}, the algorithm chooses the proper warning distance. The crucial warning distance is chosen as d_{w1} if T_{HS} is higher than T_{LS}. If not, d_{w2} is applied. However, the algorithm chooses d_{w2} if the leading vehicle's acceleration exceeds -1 m/s2 or if the leading vehicle's velocity is constant (Burgett Arthur Carter & Preziotti, n.d.).

2.4. Adaptive Cruise Control System

The Adaptive Cruise Control (ACC) System is a type of comfort system that tries to maintain speed at the predetermined level set by the driver without requiring any input from the driver while attempting to adjust other cars' road maneuvers to avoid potential crashes during this time. The hierarchical control framework of the ACC System. While low level controller seeks to implement commands from high level controller with throttle and brake inputs, high level controller wants to ascertain the configuration of the vehicles on the road and put this configuration into one of the predefined scenarios (Aksun Güvenç et al., 2006).

The system interprets the vehicle setups using various predefined scenarios. The first scenario depicts the absence of a target vehicle. After deciding on the target vehicles, more possibilities are assessed. Radar and yaw rate sensor information are used to determine whether the target vehicle is there. In contrast to distance data, which shows longitudinal movement, radar azimuth data shows lateral movement. To determine whether the investigated vehicle is on the same lane as the host vehicle or not, the upper-level controller compares the lateral movement of the vehicles around the host vehicle as determined by radar azimuth and distance data with the lateral movement of the host vehicle as determined by yaw rate sensor and velocity data. With turning target vehicles, it is possible to identify lane-changing vehicles in this manner. The longitudinal movement detection component is initiated when it is determined that a target vehicle is in the same lane as the host vehicle. The goal of this section is to identify if the target vehicle is accelerating, decelerating, or moving at a constant speed. Depending on the chosen scenario, command information is provided to the low level controller.

Using input from the throttle and brake, the low level controller attempts to achieve the desired acceleration. Using Newton's second law, desired acceleration is transformed into desired longitudinal force. The desired engine or brake torque was then generated using this longitudinal force information. Using an inverse engine model look-up table and engine angular velocity information, required engine torque is translated into desired throttle input. The desired braking pedal input is also provided by the brake model(Aksun Güvenç et al., 2006).

Launch the driving assessments first to gather data on the driver's actual lateral driving behavior. When a motorist has varied driving objectives, such as lane keeping or not, the driving parameters alter. These give the control decision layer a design foundation. Next, a joint-warning algorithm for TLC and FOD was suggested. Based on this, two databases of driver profiles and lane keeping scenes are created for an adaptive adjustment approach. The decision-making layer of LKAS was then optimized in the following stage of the work. Activation condition judgment, Driver operating status judgment, and whether the system should interfere are its three component aspects. Finally, a suggested active control technique based on EPS control was tested through simulation using the MATLAB/autonomous driving toolbox.

2.5. Research Gap

The research included in this literature review has identified several research gaps in context of protecting collision in lane departure, lane changing/merging, and overtaking. This section summarizes the identified research gaps.

A. Most literatures which apply the sensors and controllers are aimed to prevent collision in the means of alerting the driver using warning light and alarms as an actuator. This cannot guarantee the collision as the driver may not respond consciously to the warning. In addition, the driver may not distinguish the severity of the risk in different situations.

B. Some previous literatures did well-designed active-control system for the application of several low-speed vehicles. However, their implementation in the realistic high speed and serious lane-changing conditions are not considered and validated through mechanical simulations.
C. To the best of my knowledge, previous literatures which design in autonomous emergency maneuvering did not consider the vehicle dynamics of multiple vehicles in different potential driving conditions. Thus, they lack of predictive approach of relative speed, distance, acceleration and collision time.
D. Considering gap (C), literatures of various researchers who studied the vehicle dynamics and ran mechanical simulation didn't involve throttle as active safety system. It makes it difficult to guarantee the safety in all driving condition.

The intention of this thesis is in addressing the above research gaps and contribute in reducing the collision probability in avoidable lane-changing conditions. This study uses several literatures as valuable resources and develops advanced collision avoidance by combining the concept of vehicle dynamics, autonomous emergency maneuvering, adaptive cruise control, and advanced driving assistance system.

CHAPTER THREE

METHODOLOGY

3.1. System Description

Firstly, information about vehicle dynamics is collected which is related in lane-changing. Then, a vehicle dynamic model (i.e, CarSim) integrates with the MATLAB-Simulink to generate more realistic vehicle trajectories. The lane change vehicle trajectories are to be fed into CarSim and simulated by CarSim's vehicle dynamics model as shown in the figure 10. Previously modeled control system using Simulink is incorporated with CarSim to estimate the potential collision occurrence through simulations in order to take actions through active safety systems.

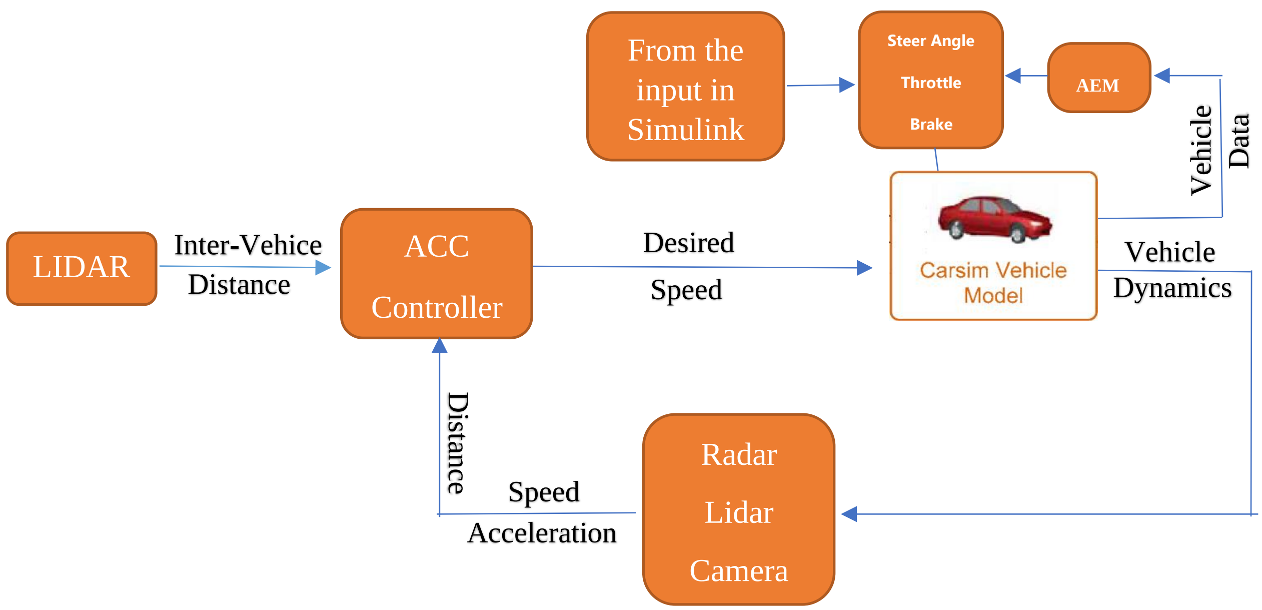

Figure 10: The architecture of the collision avoidance system

According to (Do et al., 2017), advanced overtaking calls for aggressive lane changes rather than passive ones. Three driving modes—lane-keeping mode (LK), lane change mode (LC), and lane-keeping mode for lane change (LKC)—have been developed for active lane-changing maneuvers. A flow chart for choosing the driving mode is shown in Figure 11. The ego car follows Vset or a vehicle in front of it when in lane-keeping mode. Based on the conditions of the nearby vehicles, a lane change is required when moving into an overtaking lane or moving back into a driving lane. Target space, demand, and possibility are three lane change ideas that are designed for overtaking judgments. The driving mode is chosen after three concepts have been examined.

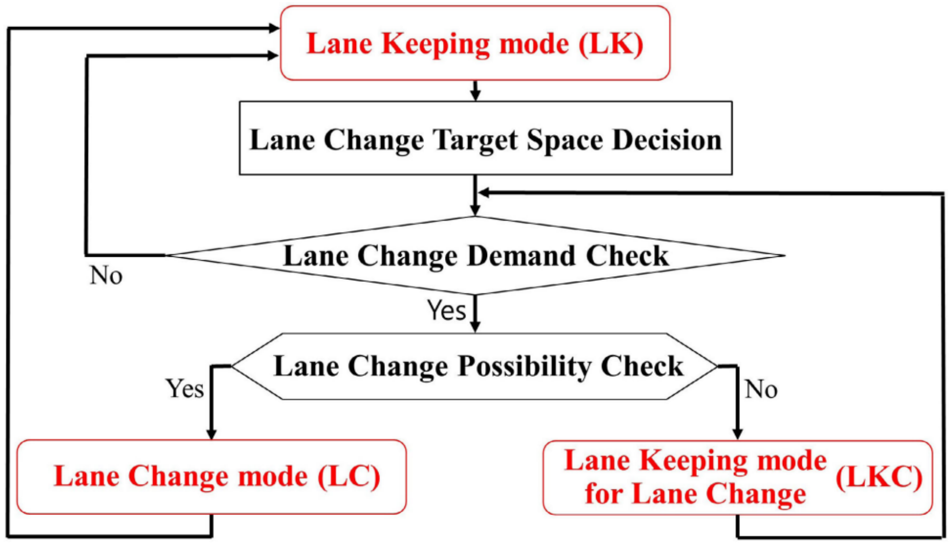

Figure 11: Flow chart of driving mode decision for overtaking(Chae & Yi, 2020)

3.2. Materials

The materials to be used for the study are listed in table 1.

Table 1: List of materials

Item	Description
MATLAB	Automated Driving Toolbox
	Model Predictive Control Algorithm
	Navigation Toolbox
	Simulink
	Sensor Fusion and Tracking Toolbox
CARSIM	Mechanical Simulation Software

3.3. Methods

- The decision interpretation is analyzed by target check, demand check and possibility check calculations.
- The vehicle dynamics is evaluated with bicycle model which is imported on Simulink on later on to develop the control algorithm.

- The simulation takes place repeatedly till best result is gained. Corrections are made in the sensors and actuator arrangement until it is validated through the safest simulation result. The possible speed ranges are also identified to understand in what situations and vehicle types that the design could be implemented.
- The three driving modes (normal, aggressive and conservative) analyzed and applied to the system.
- The control system is analyzed including trajectory generation and path tracking with computational method.
- Finally, all systems will be merged and run to obtain result.
- The results is assessed and verified whether it is obtained as predicted or not.

The work flow of the proposed model is illustrated on Figure 12

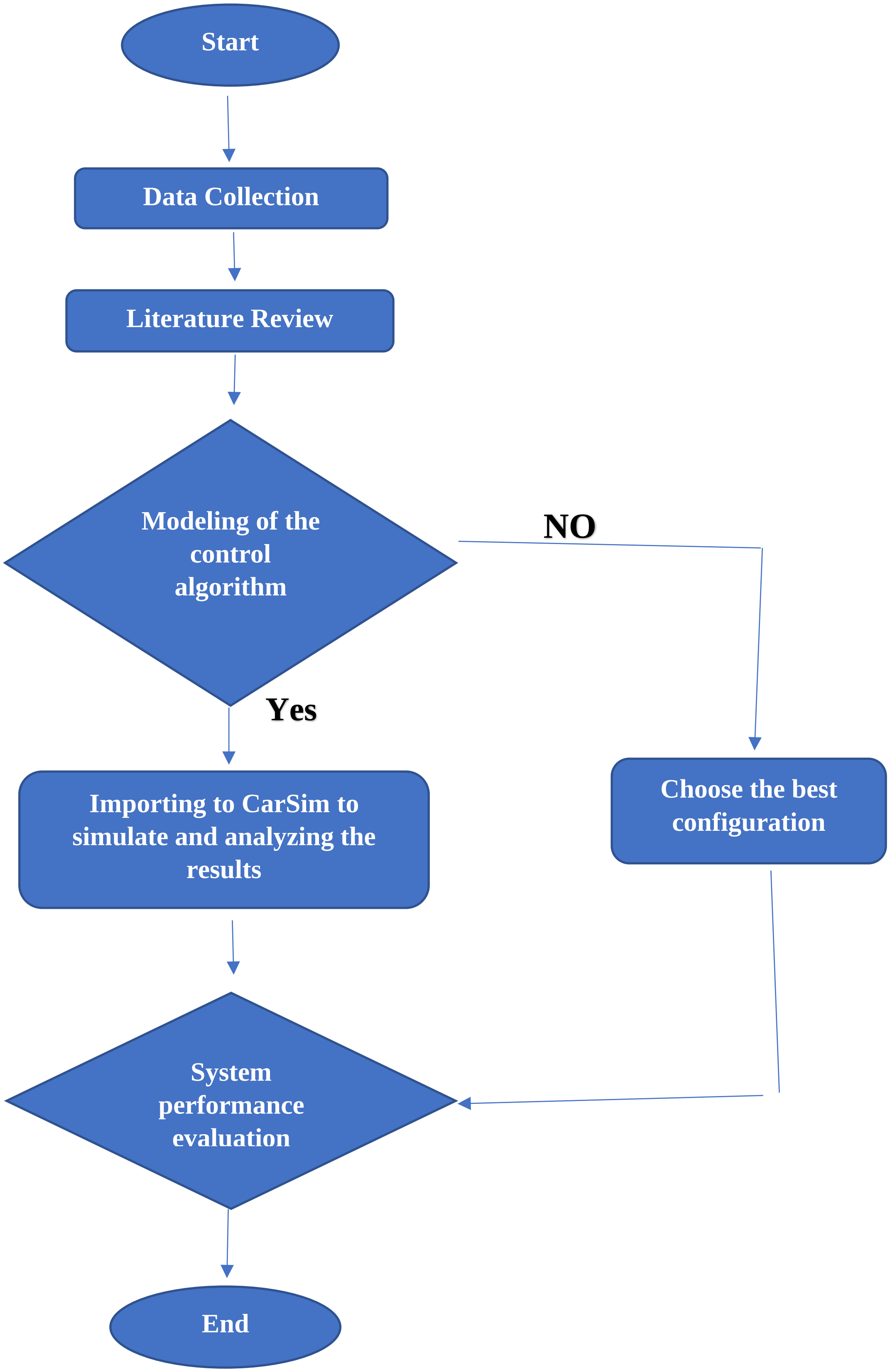

Figure 12: The workflow of the model design

3.4. Lane Change Target Space Decision

Checking the status of side cars on the target lane is the first stage in choosing the driving mode for lane changes. 'Target space' is a concept that has been developed in this paper. Target space refers to the area between the cars in the target lane where a lane change can be made. Candidates for the target space are identified before the target space is chosen. As seen in Figure 13, by applying S_{dc} to the virtual targets and identified vehicles in the target lane, space candidates for lane changes might be produced. Two space candidates are created by one side vehicle. Each applicant for a space has a 'j' index. Each space's position and velocity rely on the vehicle's internal state at the time it was created. To locate the best space for a lane shift, it is necessary to suppose that the other car will exhibit a variety of behaviors because it may accelerate and decelerate for an active lane change. The ego vehicle is said to have a number of contenders for acceleration. The contenders for acceleration have a fixed minimum value. Depending on the preceding vehicle, the acceleration candidates' maximum value varies. Between the highest and least acceleration, several acceleration candidates are derived. According to acceleration candidates, the ego vehicle's expected behavior is predicted. The following describes the assumed behavior:

$$v_i(n+1) = v_i(n) + a_i(n) \times t_{sam} \quad (3.1)$$

$$p_i(n+1) = p_i(n) + v_i(n) \times t_{sam}$$

where subscript i is the i-th acceleration candidate.

Among the potential spaces, a target space must be chosen. The target space is chosen based on two conditions. These requirements are drawn from the lane-change determination rule used by human drivers. In order to change lanes, drivers do not aim to enter a space that is either too wide or too narrow. The ego vehicle's arrival time in space is the first need. The distance between successive space candidates is the second requirement. In order to choose the target space, an optimization problem is developed. As the target space, the candidate with the lowest cost is chosen. The optimization challenge looks like this:

$$\min_{i,j} J_{ij} = \frac{T_{ij}}{C_j}, \quad (3.2)$$

$$s.t\ \ T_{ij} = \frac{p_{ij}}{v_{ij}},$$

$$p_{ij=} \sum_{n=1}^{N_p} \frac{p_j(n) - p_i(n) \pm sd_{c,j}(n)}{N_p}, \tag{3.3}$$

$$v_{ij=} \sum_{n=1}^{N_p} \frac{v_j(n) - v_i(n)}{N_p},$$

$$c_{j=} \sum_{n=1}^{N_p} \frac{p_{j+1}(n) - P_j(n)}{N_p},$$

3.5. Lane Change Demand Check

Choosing which data from the adjacent lane is used is crucial when deciding if overtaking will take place. Traffic flow has been used in earlier research to help in overtaking decisions. According to earlier study, traffic flow can be divided into microscopic and macroscopic viewpoints (K. Li & Ioannou, 2004). The tiny point of view has been used in overtaking choices because local sensors of the ego vehicle could only measure a small region (Suh et al., 2018). In a perfect world, it makes sense to base overtaking decisions on traffic flow. On a real road, though, side vehicles travel at different speeds. Drivers make their overtaking decisions based less on the average speed of the target lane and more on the velocity of the space they will be moving into. As a result, in this study, overtaking judgments are made using the target space described above. The decision process makes use of the vehicle's speed as it approaches the target area. Target space velocity (v_{space}) is the designation given to the speed.

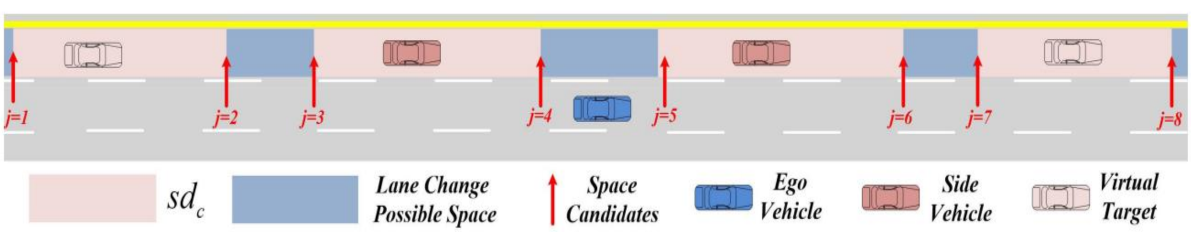

Figure 13:. Space candidates for lane change based on sd_c(Chae & Yi, 2020)

When v_{space} is compared to the speed of the vehicle in front (v_{prc}), lane change is demanded.

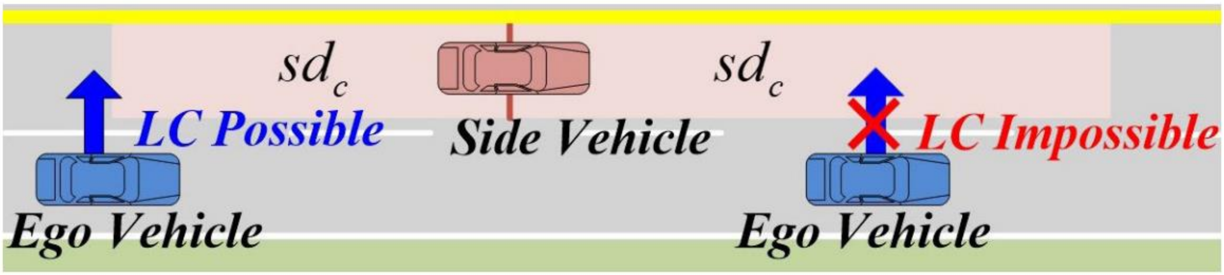

Figure 14. A concept of lane change possibility based on safe distance (Chae & Yi, 2020).

It is necessary to switch lanes twice when overtaking. Once when the sluggish preceding car is encountered by the ego vehicle. This situation calls for a lane change to the overtaking lanes. Another is when the ego vehicle transitions back to the driving lane after leaving the overtaking lane. Driving lanes are required to change lanes in this situation. Different circumstances are therefore required for two reasons. The condition known as "enter (to the overtaking lane)" is

defined as:

$$v_{prc} < v_{set} \wedge v_{prc} < v_{space} \tag{3.4}$$

The return (to the driving lane) condition is defined as follows:

$$v_{set} \leq v_{space} \vee v_{prc} < v_{x,space} \tag{3.5}$$

3.6. Lane Change Possibility Check

The driving mode switches from LK to LKC or LC when a lane change is required. The ego vehicle must assess the likelihood of the lane shift based on the sdc of side vehicles before choosing which mode to use between LKC mode and LC mode. The inability to change lanes is caused by any side car that is positioned closer than sdc. An illustration of the potential lane change is shown in Figure 11. A lane change is possible when the relative positions of side cars are greater than the sdc of each vehicle in the whole prediction horizon. When a lane change is available, the LC mode is activated. The probability of a lane change is continually examined, even when the vehicle is in lane change mode. The possibility has been checked until the ego vehicle crosses the lane. The condition of the lane change possibility is given by:

$$|p_{ms}| > |sd_{c,ms}| \tag{3.6}$$

where Nms is the total number of side cars and subscript ms denotes the ms-th side vehicle on the target lane (m = 1,..., Nms). Every prediction horizon is tested for the condition for every side vehicle found on the target lane. If any of the conditions related to all checks are not met, LC mode will not begin. In this instance, LKC mode is maintained.

3.7. Vehicle Dynamics

3.7.1. Vehicle Model

Under the premise of a constant tire normal load, that is, F_{zf}, F_{zr}=constant, the dynamics of the car are modeled using a "bicycle model" (Falcone et al., 2007). The vehicle model in Fig. 1 is shown in diagram form and has the following degrees of freedom for longitudinal, lateral, and turning or yaw:

$$\mathrm{m}\ddot{x} = \mathrm{m}\dot{y}\dot{\psi} + 2F_{xf} + 2F_{xr} \tag{3.6a}$$

$$\mathrm{m}\ddot{y} = \mathrm{m}\dot{x}\dot{\psi} + 2F_{xf} + 2F_{xr} \tag{3.6b}$$

$$\mathrm{I}\,\ddot{\psi} = 2\mathrm{a}F_{yf} + 2\mathrm{b}F_{yr} \tag{3.6c}$$

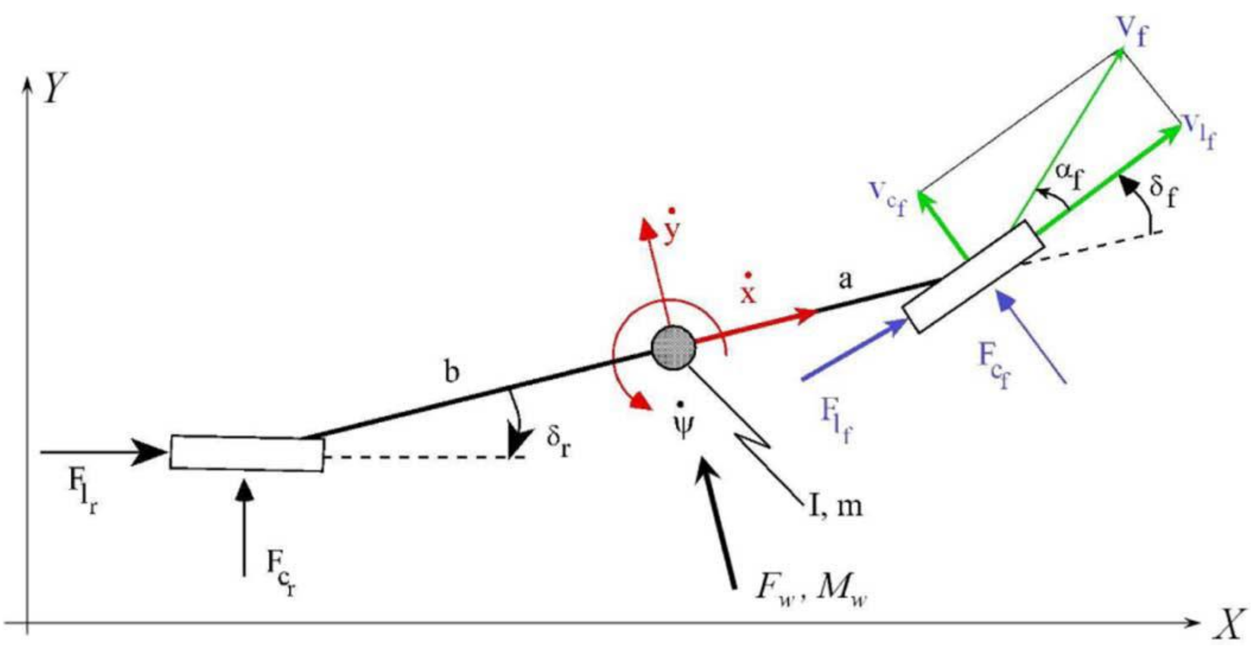

Figure 15: Simplified vehicle Bicycle Model (Falcone et al., 2007)

The equations of motion for the vehicle in an absolute inertial frame are

$$\dot{X} = \dot{x}\cos\psi - \dot{y}\sin\psi, \qquad \dot{Y} = \dot{x}\sin\psi + \dot{y}\cos\psi \tag{3.7}$$

Equations of motion for the wheel's lateral (or cornering) and longitudinal wheel velocities are provided.

$$v_{lf=}v_{yf}sin\delta_f + v_{xf}cos\delta_f \tag{3.8a}$$

$$v_{lr=}v_{yr}sin\delta_r + v_{xr}cos\delta_r \tag{3.8b}$$

$$v_{cf=}v_{yf}cos\delta_f - v_{xf}sin\delta_f \tag{3.8c}$$

$$v_{cr=}v_{yr}cos\delta_r + v_{xr}cos\delta_r \tag{3.9d}$$

where δ_f and δ_r are front and rear wheel steering angle, respectively, and

$$v_{yf} = \dot{y} + a\dot{\psi}, \qquad v_{yr} = \dot{y} - b\dot{\psi} \tag{3.10a}$$

$$v_{xf} = \dot{x}, \qquad v_{xr} = \dot{x} \tag{3.10b}$$

By using the corresponding subscript for each variable, the following equations hold for both the rear and front axes. The center of gravity is subject to the following forces as a result of longitudinal and lateral tire forces:

$$F_{y=}F_l\sin\delta + F_c\cos\delta, \quad F_{x=}F_l\cos\delta - F_c\sin\delta \tag{3.11a}$$

The tire forces F_l and F_c for each tire are given by

$$F_l = f_l(\alpha, s, \mu, F_z), \qquad F_c = f_c(\alpha, s, \mu, F_z) \tag{3.11b}$$

where $\alpha, s, \mu\ and F_z$ are defined next. The angle between the wheel velocity vector and the direction of the wheel itself, known as the tire slip angle, can be stated succinctly as

$$\alpha = \arctan\frac{v_c}{v_l} \tag{3.12}$$

The slip ratio is defined as

$$F_l = f_l(\alpha, s, \mu, F_z), \qquad F_c = f_c(\alpha, s, \mu, F_z)$$

$$s = \begin{cases} \frac{r\omega}{v_l} - 1, if\ v_l > r\omega, v_1 \neq 0\ for\ braking \\ 1 - \frac{v_1}{r\omega},\ if\ v_1 < r\omega, \omega \neq 0\ for\ driving \end{cases} \tag{3.13}$$

where the wheel's radius and angular speed, respectively, are denoted by r and ω. The front and back wheels of a vehicle are believed to have an equal road friction coefficient, represented by the parameter. dependent on the geometry of the automobile model (specified by the parameters a and b), is the total vertical load of the vehicle and is distributed between the front and rear wheels.

$$F_{zf} = \frac{bmg}{2(a+b)} \quad , \qquad F_{zr} = \frac{amg}{2(a+b)} \tag{3.14}$$

The nonlinear vehicle dynamics described in (1)–(9), can be rewritten in the following compact from:

$$\frac{d\xi}{dt} = f_s(t), \mu(t)(\xi(t), u(t)) \tag{3.15}$$

where the dependence on slip ratio and friction coefficient value at each time instant has been explicitly highlighted. The state and input vectors are $\xi = [\dot{y}, \dot{x}, \psi, \psi, \dot{Y}, X]^l and\ u = \delta_f$ respectively. In this paper, δ_r is assumed to be zero at any time instant.

3.7.2. Tire Model

The forces that determine how a vehicle handles are all produced by the tires, with the exception of gravity and aerodynamic forces. Tire forces are the main external factor, and because of their highly nonlinear behavior, they significantly alter the longitudinal and lateral maneuvering range of a vehicle's handling characteristics. Therefore, it is crucial to employ a realistic nonlinear tire model, especially when researching significant control inputs that produce responses that are close to the vehicle's maximum range of maneuverability. Large values of slip ratio and slip angle may be present at the same time under such circumstances because the lateral and longitudinal motions of the vehicle are closely connected through the tire forces. The vast majority of tire models currently in use are "semi-empirical" in nature. In other words, essential parameters are dependent on tire data readings, and the structure of the tire model is determined by analytical considerations. These models range from very straightforward (where lateral forces are calculated as a function of slip angle, based on one observed slope at α=0 and one measured value of the highest lateral force) to somewhat complex algorithms, which make use of tire data collected at various loads and slip angles. In this study, we explain the longitudinal and cornering forces of the tire using the Pacejka tire model (Bakker et al., 1987). The interplay between the longitudinal force and the cornering force in combined braking and steering is taken into account by this intricate, semi-empirical nonlinear model. It is presumpted that the normal force, slip angle, surface friction coefficient, and longitudinal slip all affect the longitudinal and cornering forces. For fixed values of the friction coefficients, Fig. 16 shows longitudinal and lateral forces vs longitudinal slip and slip angle. We point out that the "bicycle" model's front tire corresponds to the two front tires of a real car.

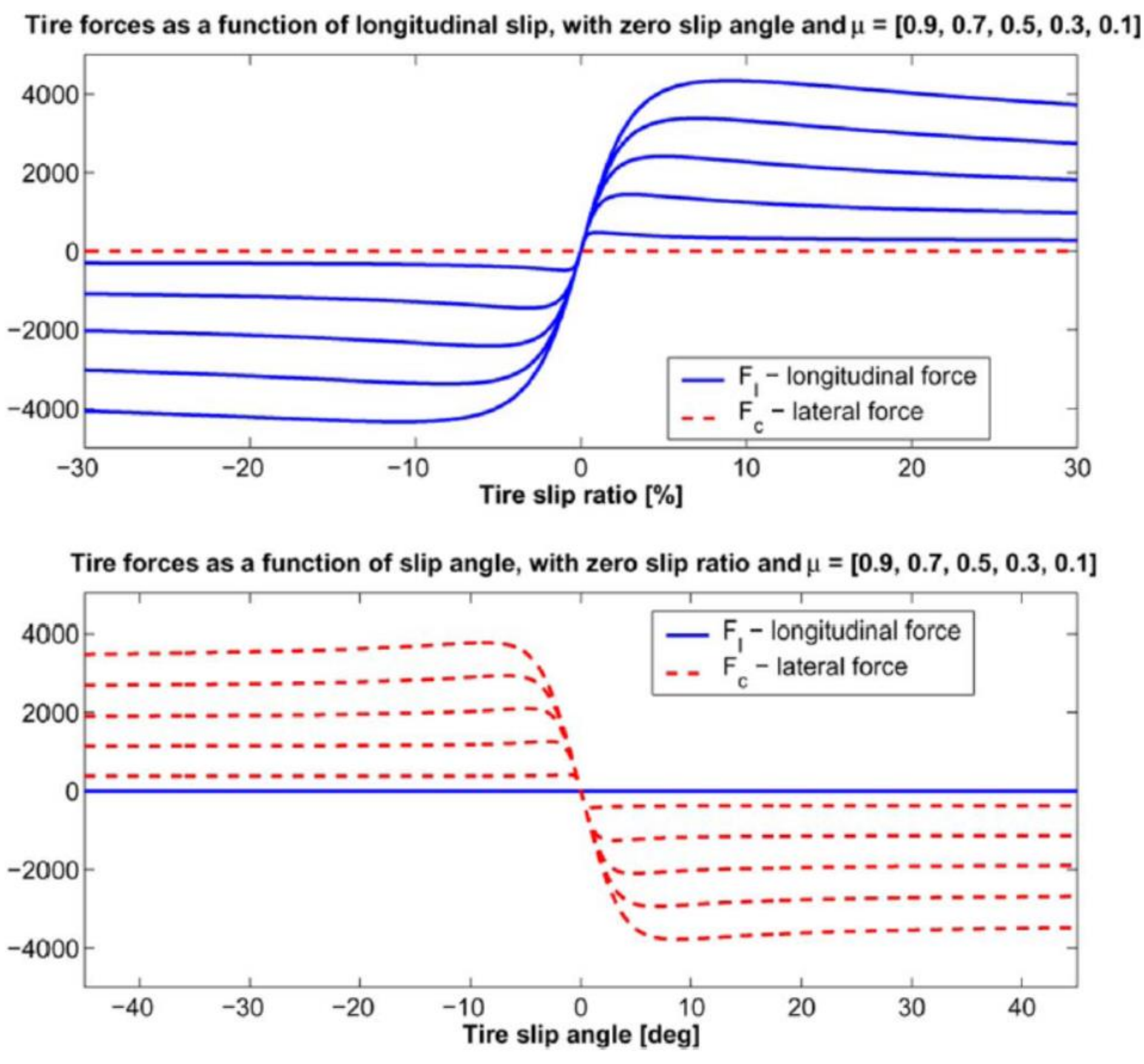

Figure 16. Longitudinal and lateral tire forces with different μ coefficient values(Falcone et al., 2007).

3.7.3. Vehicle Model with Electrically Powered Steering

A classical fourth-order linear model, sometimes known as the "bicycle model" (Fig. 15), was employed because this study is primarily concerned with the lateral control of a vehicle (Ackermann et al., 1995). Since this work is concerned with highway driving, it is practical to ignore the effects of road curvature and assume that the route is straight. A DC motor installed on the steering column, for which a second order model was used, supplies the steering torque required for the assistance. The model of the vehicle, including the model with electrical steering assistance, is given by:

$$\dot{x} = A.x + \boldsymbol{B}.(T_a + T_d) \tag{3.16}$$

$$A = \begin{bmatrix} a_{11} & a_{12} & 0 & 0 & b_1 & 0 \\ a_{21} & a_{22} & 0 & 0 & b_2 & 0 \\ 0 & 1 & 0 & 0 & 0 & 0 \\ v & l_s & v & 0 & 0 & 0 \\ 0 & 0 & 0 & 0 & 0 & 1 \\ \frac{T_{s\beta}}{l_s R_s} & \frac{T_{sr}}{l_s R_s} & 0 & 0 & -\frac{2K_p c_f \eta_t}{l_s R_s^2} & -\frac{\beta_s}{l_s} \end{bmatrix} \tag{3.17}$$

$$B = \left(0,0,0,0,0,\frac{1}{R_s I_s}\right)^T \tag{3.18}$$

Where

$$a_{11} = -\frac{2(c_r + c_f)}{mv}, \qquad a_{12} = -1 + \frac{2(l_r c_r + l_f c_f)}{mv^2} \tag{3.19}$$

$$a_{21} = \frac{2(I_r c_r + I_f c_f)}{J}, \qquad a_{22} = -\frac{2({I_r}^2 c_r + {I^2}_f c_f)}{Jv}$$

$$c_r = c_{r0}\mu \qquad c_f = c_{f0}\mu$$

$$b_1 = \frac{2c_f}{mv} \qquad b_2 = \frac{2c_f I_f}{J}$$

$$T_{s\beta} = \frac{2K_p C_f \eta_t}{R_s} \qquad T_{sr} = \frac{2K_p C_f I_f \eta_t}{R_s v}$$

The definitions and the numerical values of the above parameters are given at the end of the paper. The state vector is x , $(\beta, r, \psi L, yL, \delta f, \dot{\delta} f)^{T}$, where β denotes the side slip angle, r is the yaw rate, ψ_L is the relative yaw angle, y_L is the lateral offset with respect to the lane centerline at a look-ahead distance l_S, δf is the steering angle, and $\dot{\delta}_f$ is its derivative. The inputs for the system given in Eq. (3.16) are the driver's torque Td and the assistance torque Ta. The whole state vector is considered to be available for measurement.

At the end of the paper, the definitions and numerical values for the aforementioned parameters are provided. The state vector is represented by the equation $\mathbf{x} \triangleq (\beta, r, Y_L, \psi_L, \delta_f, \dot{\delta}_f)^T$,where represents the side slip angle, r is the yaw rate, L is the relative yaw angle, yL is the lateral offset with respect to the lane centerline at a look-ahead distance l_S, δ_f is the steering angle, and f is its derivative. The driver's torque T_d and the assistance torque T_a serve as the system's inputs in Eq. (3.16). The entire state vector is seen as being measurable.

3.8. Driver Model

In order to reduce the lateral positional divergence between the preview point and the projected point in the route tracking, a human driver constantly acts as a steering controller. The driver model with a single preview point30 is used in this paper. Figure 17 illustrates this model's fundamental idea.

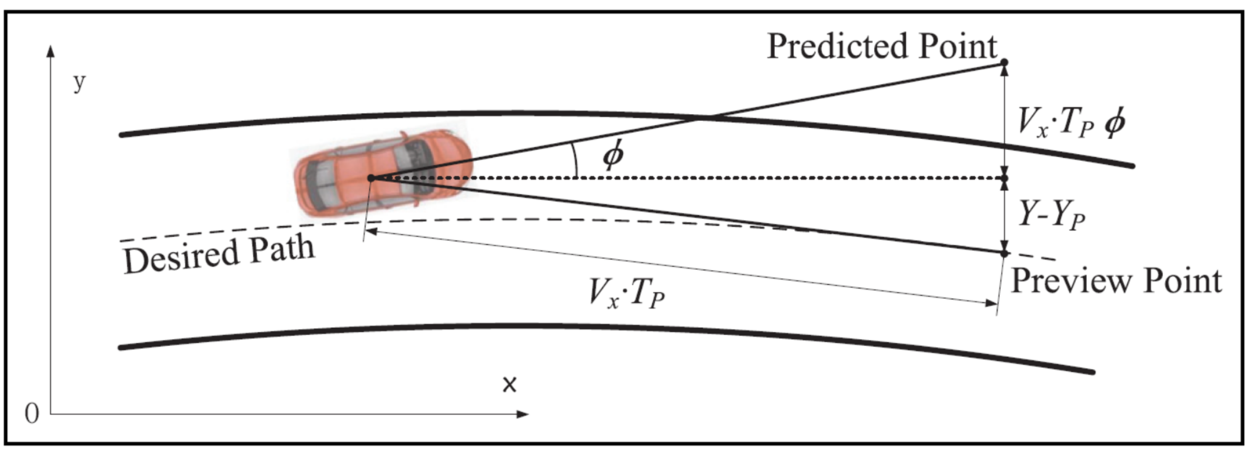

Figure 17. The principle of the driver model(Zhang et al., 2019).

The following is a description of the driver model under the modest heading angle assumption.

$$\ddot{\delta} = -\frac{1}{a_0 T_d^2}\delta - \frac{1}{a_0 T_d}\dot{\delta} + \frac{R_g G_h}{a_0 T_d^2}\left[Y_p - (Y + V_x T_p \phi\right] \quad (3.20)$$

where δ represents the front tires' steering angle; Rg is the steering system's gear ratio; Y and Y_P stand for the current point's and the preview point's respective lateral positions; Vx denotes longitudinal velocity, ϕ denotes heading angle, while T_P and Td denote, respectively, the driver's preview time and delay time. A_0 is a constant, and G_h is the steering proportional gain. The values of T_P, T_d, a_0, and Gh depend on the properties of the driver(Macadam, 2003). In the same situation, different drivers may perform differently depending on factors like steer proportional gain and time delay.28 A driver who is older, for instance, likes to react with a smaller Gh and a greater T_d, while a motorist who is younger has the opposite reactions. This is because being older may damage one's physical capability (Wang et al., 2017).

Considering different driving characteristics, the parameters of driver model are presented in Table I (Wang et al., 2017),(Dai et al., 2017).

Table 2. Parameters For Various Driving Styles

Parameters	Driving Styles		
	Aggressive	Normal	Conservative
T_d	0.14	0.18	0.24
T_p	1.02	0.94	0.83
G_s	0.84	0.75	0.62
a	0.24	0.23	0.22

3.9. Control System

3.9.1. Simplified Dynamic Model

For controller design, a streamlined dynamic model of the 4WS AGV is constructed in this part. In order to do this, only lateral and yaw motions in the horizontal plane are taken into consideration, ignoring pitch and roll motions. It is anticipated that the longitudinal velocity of the 4WS AGV would remain constant. Figure 18 depicts the 2 DoF simplified planar motion model as a consequence.

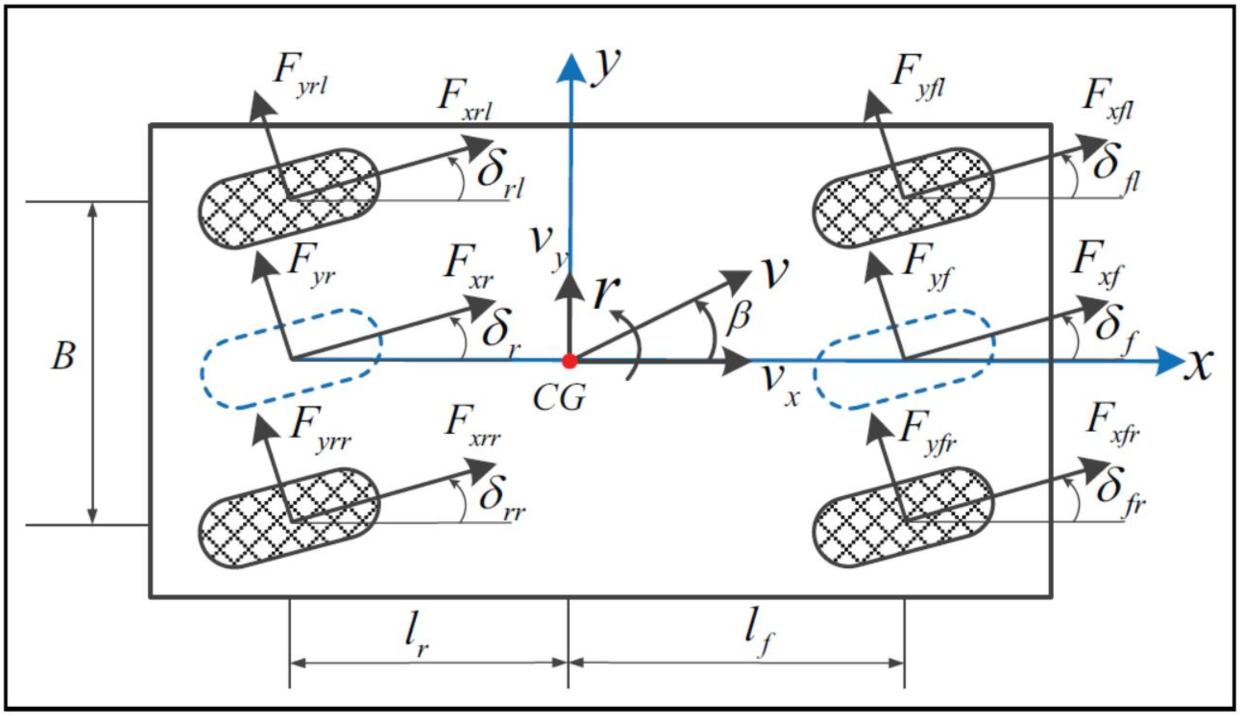

Figure 18. Planar motion model of 4WS AGV(Hang & Chen, 2021).

Additionally, the four-wheeled planar motion model can be condensed into a simpler single-track model with two wheels, which is shown by the blue model in Figure 2. The center of gravity (CG) of the 4WS AGV serves as the fixed reference frame for the body. The longitudinal force and lateral force of each tire are denoted by the symbols F_{xi} and F_{yi}, respectively (where i = *fl, fr, rl, rr, f, r)*. The longitudinal and lateral velocities are denoted by v_x and v_y, respectively. The CG sideslip angle and yaw rate are denoted as β and r.

The steering angle relationship in the two models should satisfy the Ackerman steering geometry, which can be expressed as follows:

$$\begin{cases} \tan\delta_{fl} = \dfrac{\tan\delta_f}{1-\frac{B}{2l}(\tan\delta_f - \tan\delta_r)} \\ \tan\delta_{fr} = \dfrac{\tan\delta_f}{1+\frac{B}{2l}(\tan\delta_f - \tan\delta_r)} \\ \tan\delta_{rl} = \dfrac{\tan\delta_r}{1-\frac{B}{2l}(\tan\delta_f - \tan\delta_r)} \\ \tan\delta_{rr} = \dfrac{\tan\delta_r}{1+\frac{B}{2l}(\tan\delta_f - \tan\delta_r)} \end{cases} \tag{3.21}$$

where δ_i (i = fl, fr, rl, rr, f, r) denotes the steering angle of each wheel. The lateral dynamic model of 4WS AGV can be derived as follows using Newton's Second Law.

$$a_y = \dot{v}_y - v_x r = \frac{1}{m}(F_{yf}\cos\delta_f + F_{yr}\cos\delta_r + F_{xf}\sin\delta_f + F_{xr}\sin\delta_r) \tag{3.22}$$

where a_y stands for the 4WS AGV's CG lateral acceleration. Additionally, the 4WS AGV's yaw dynamic model can be stated as

$$\dot{r} = \frac{1}{I_z}(l_f F_{yf}\cos\delta_f - l_r F_{yr}\cos\delta_r + l_f F_{xf}\sin\delta_f - l_r F_{xr}\sin\delta_r) \tag{3.23}$$

It results in cos $\delta_i \approx 1$ and sin $\delta_i \approx 1$, assuming that the steering angles of a car's wheels are relatively modest at high speeds. Consequently, equations (3.22) and (3.23) can be reduced to

$$a_y = \dot{v}_y - v_x r = \frac{1}{m}(F_{yf} + F_{yr}) \tag{3.24}$$

$$\dot{r} = \frac{1}{I_z}(l_f F_{yf} - l_r F_{yr}) \tag{3.25}$$

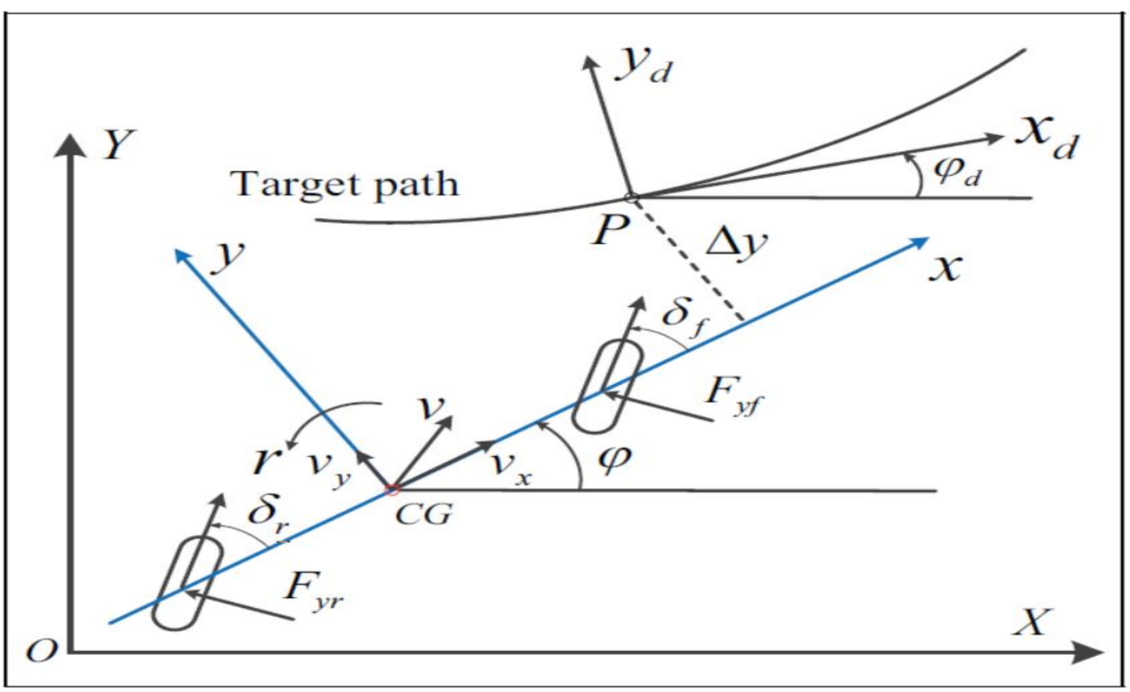

Figure 19: Path tracking model of 4WS AGV(Hang & Chen, 2021)

The tire slip angles can be thought of as being very small because it is anticipated that the steering angles of a vehicle's wheels are very small at high speeds. Thus, it is possible to establish the linear relationship between the lateral tire force and tire slip angle, which can be written as

$$F_{yf} = -k_f\alpha_f, \quad F_{yr} = -k_r\alpha_r \tag{3.26}$$

While tire slip angles are defined as:

$$\alpha_f = \frac{v_y + l_f r}{v_x} - \delta_f, \quad \alpha_r = \frac{v_y - l_r r}{v_x} - \delta_r \tag{3.27}$$

Equations (3.26) and (3.27) can be substituted for equations (4) and (5) to produce the following linear dynamic model of 4WS AGV.

$$\dot{v}_y - v_x r = -\frac{k_f + k_r}{m v_x} v_y - \frac{l_f k_f - l_r k_r}{m v_x} r + \frac{k_f}{m}\delta_f + \frac{k_r}{m}\delta_r \tag{3.28}$$

$$\dot{r} = -\frac{l_f k_f - l_r k_r}{I_z v_x} v_y - \frac{l_f^2 k_f + l_r^2 k_r}{I_z v_x} r + \frac{l_f k_f}{I_z}\delta_f - \frac{l_r k_r}{I_z}\delta_r$$

3.9.2. Path Tracking Model

Based on the single-track model in Figure 2 and the 4WS AGV route tracking model, which is presented in Figure 18, the path tracking controller is designed. The vehicle's direction on its intended course is indicated by the xy, $x_d\, y_d$ coordinate frame in addition to the body coordinate frame XY, and the geodetic coordinate system is represented by the xy coordinate frame. The yaw angle error $\Delta\varphi$ and the lateral position error Δy must be minimized in order to solve the 4WS AGV route tracking problem.

The yaw angle error $\Delta\varphi$ can be expressed as

$$\Delta\varphi = \varphi - \varphi_d \tag{3.29}$$

Where φ_d is the target yaw angle and its derivative can be written as:

$$\dot{\varphi}_d = \frac{\dot{x}}{R_d} \tag{3.30}$$

Where R_d is the curvature radius of the target path.

Taking the derivative with respect to time on both sides of equation (3.29) yields that

$$\Delta\dot{\varphi} = \dot{\varphi} - \dot{\varphi}_d = \dot{\varphi} - \frac{\dot{x}}{R_d} \tag{3.31}$$

The lateral position error Δy is defined as the vertical distance from the target path point P to x axis, and its second derivative can be written as:

$$\Delta\ddot{y} = a_y - a_{yd} \tag{3.32}$$

Where a_{yd} is the target lateral acceleration and can be expressed as:

$$a_{yd} = \frac{\dot{x}^2}{R_d} = \dot{x}\dot{\varphi}_d \tag{3.33}$$

Furthermore, equation (3.32) can be written as

$$\Delta\ddot{y} = \ddot{y} + \dot{x}\dot{\varphi} - \dot{x}\dot{\varphi}_d = \ddot{y} + \dot{x}\Delta\dot{\varphi} \tag{3.34}$$

Integrating equation (14), which results in the assumption that the longitudinal velocity is constant, reveals that

$$\Delta\dot{y} = \dot{y} + \dot{x}\Delta\varphi \tag{3.35}$$

The following path tracking model can be developed from the aforementioned equations

$$\begin{aligned}\Delta\ddot{y} = & -\frac{k_f + k_r}{mv_x}\Delta\dot{y} - \frac{l_f k_f - l_r k_r}{mv_x}\Delta\dot{\varphi} + \frac{k_f + k_r}{m}\Delta\varphi \\ & + \frac{k_f}{m}\delta_f + \frac{k_r}{m}\delta_r - \left(\frac{l_f k_f - l_r k_r}{mv_x} + v_x\right)\dot{\varphi}_d\end{aligned} \tag{3.36}$$

$$\Delta\ddot{\varphi} = -\frac{l_f k_f - l_r k_r}{I_z v_x}\Delta\dot{y} - \frac{l_f^2 k_f + l_r^2 k_r}{I_z v_x}\Delta\dot{\varphi} + \frac{l_f k_f - l_r k_r}{I_z}\Delta\varphi$$
$$+ \frac{l_f k_f}{I_z}\delta_f - \frac{l_r k_r}{I_z}\delta_r - \frac{l_f^2 k_f + l_r^2 k_r}{I_z v_x}\dot{\varphi}_d - \ddot{\varphi}_d$$

Furthermore, a state-space version of the path tracking model is rewritten.

$$\begin{aligned} \dot{X}_c &= AX_c + BU + EW \\ Y_c &= CX_c + DU \end{aligned} \tag{3.37}$$

where the state vector$X_c = [\Delta y \quad \Delta\dot{y} \quad \Delta\varphi \quad \dot{\varphi}]^T$, control vector $U = \left[\delta_f \quad \delta_r\right]^T$, external input vector $W = \left[\dot{\varphi}_d \quad \ddot{\varphi}_d\right]^T$, and the coefficient matrices are given by

$$A = \begin{bmatrix} 0 & 1 & 0 & 0 \\ 0 & -\frac{k_f + k_r}{m v_x} & \frac{k_f + k_r}{m} & -\frac{l_f k_f - l_r k_r}{m v_x} \\ 0 & 0 & 0 & 1 \\ 0 & -\frac{l_f k_f - l_r k_r}{I_z v_x} & \frac{l_f k_f - l_r k_r}{I_z} & -\frac{l_f^2 k_f + l_r^2 k_r}{I_z v_x} \end{bmatrix} B = \begin{bmatrix} 0 & 0 \\ \frac{k_f}{m} & \frac{k_r}{m} \\ 0 & 0 \\ \frac{l_f k_f}{I_z} & -\frac{l_r k_r}{I_z} \end{bmatrix}$$

$$C = I_{4\times4} \quad and\ D = 0_{2\times2} \quad , \quad E = \begin{bmatrix} 0 & 0 \\ -(\frac{l_f k_f - l_r k_r}{m v_x} + v_x) & 0 \\ 0 & 0 \\ -\frac{l_f^2 k_f + l_r^2 k_r}{I_z v_x} & -1 \end{bmatrix}$$

3.9.3. Design of Path Tracking Controller

The 4WS AGV's control system architecture is depicted in Figure 4. The two primary components of the control system are discovered to be longitudinal motion control and path tracking control. Since longitudinal motion control is not the focus of this article's study, it won't be discussed here; readers can find it in earlier work(Hang et al., 2018). The path tracking algorithm design is the main subject of this thesis. The inputs of the path tracking controller are set to include the 4WS

AGV's real position and the target path data. After that, the path tracking controller may calculate the steering angles δ_f and δ_r. Each wheel's steering angle can be calculated and sent to the ECU using Ackerman steering geometry. Four SBW systems are controlled by the ECU to track the desired steering angle. The 4WS AGV then be able to implement path tracking control.

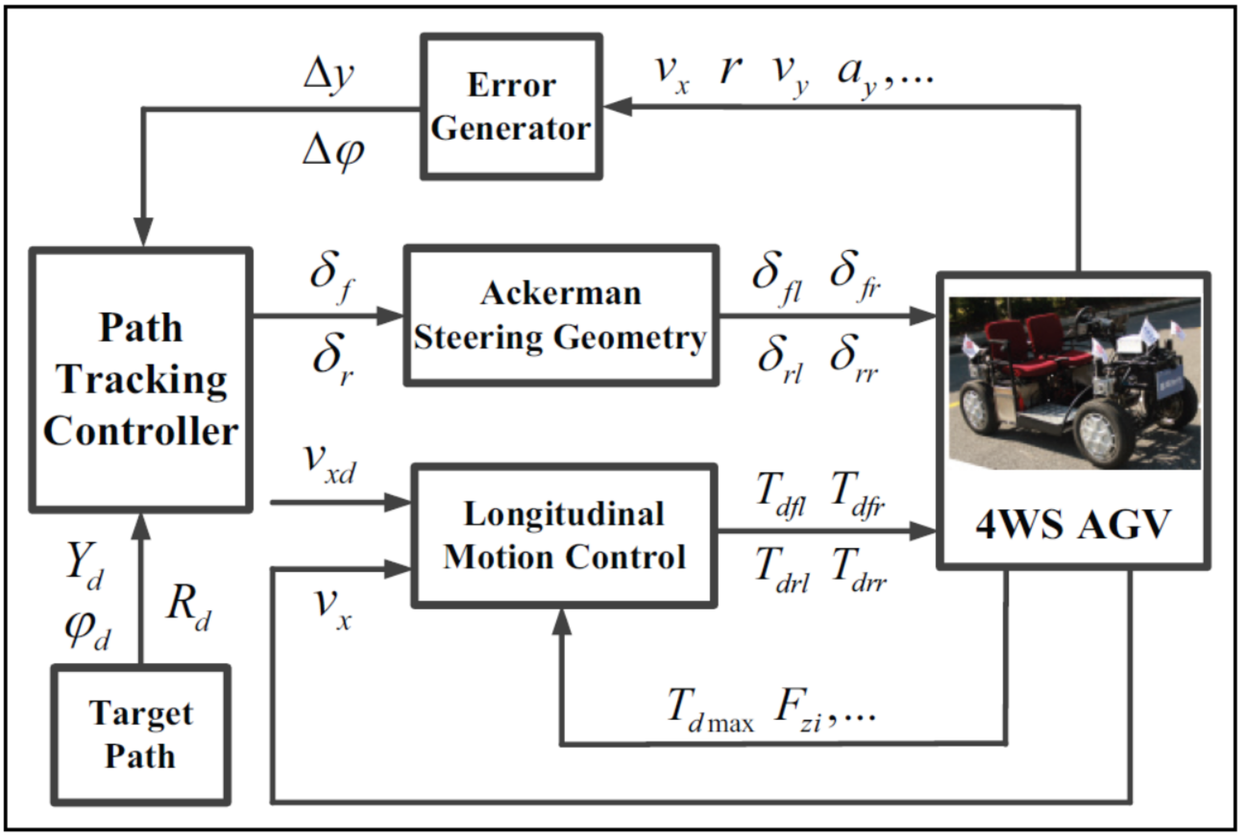

Figure 20: Control system structure of 4WS AGV(Hang & Chen, 2021).

CHAPTER FOUR

OVERVIEW OF SIMULATION SCENARIOS

4.1. The Ego Vehicle

Initially, a vehicle model of C-Class Hatchback is selected which can be served as an ego vehicle in which the control algorithm is implemented on it. The default configuration of the ego vehicle is listed in the CarSim as it is indicated on figure 21.

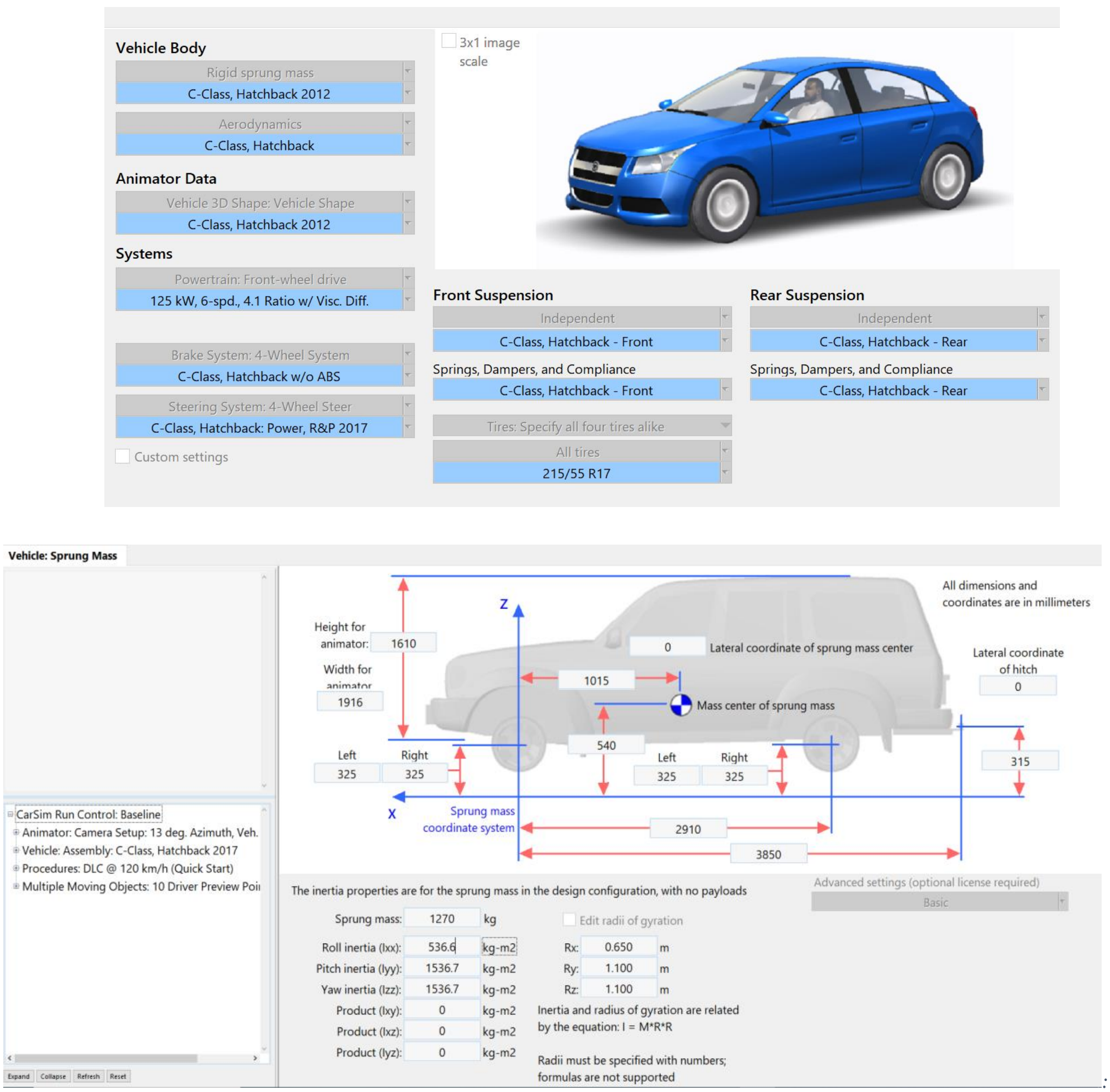

Figure 21: The initial design configuration of C-Class Hatchback

Then, suggested parameters such as: yaw moment of inertia, steering angle, cornering stiffness, l_f, l_r , and longitudinal acceleration tracking time constants is uploaded on Simulink(as showed on figure 22), which is going to be imported on CarSim later on.

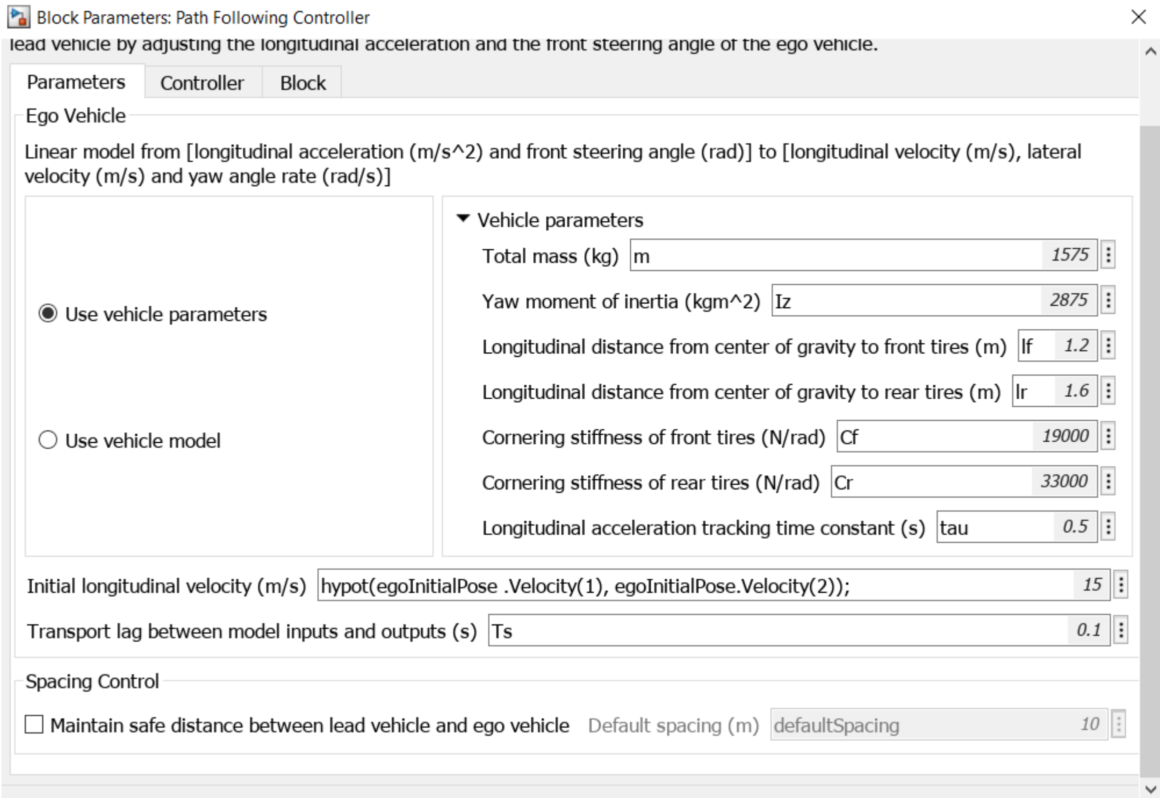

Figure 22: The Ego vehicle parameters which is uploaded on Simulink initially

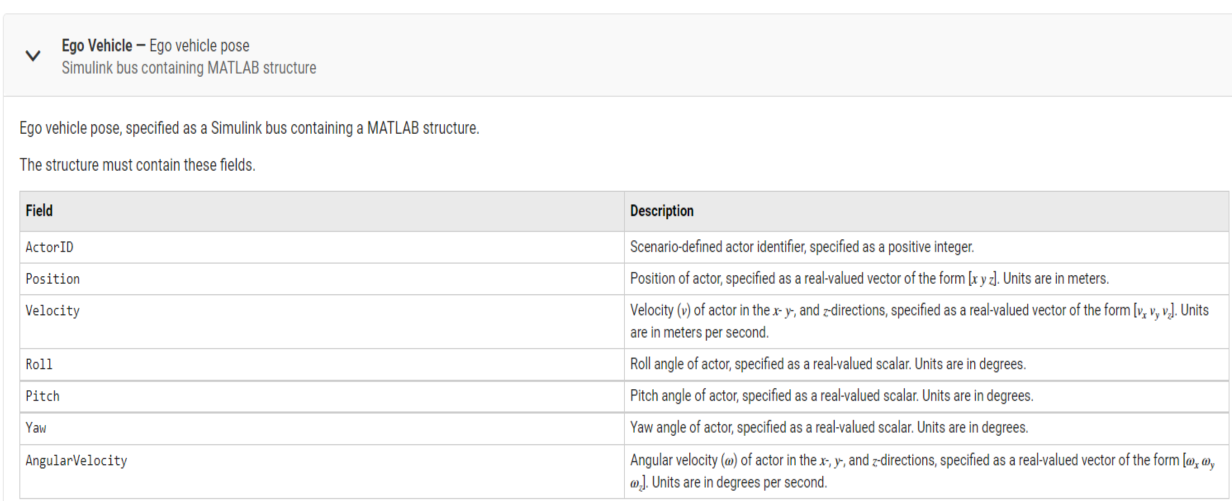

Ego Vehicle — Ego vehicle pose
Simulink bus containing MATLAB structure

Ego vehicle pose, specified as a Simulink bus containing a MATLAB structure.

The structure must contain these fields.

Field	Description
ActorID	Scenario-defined actor identifier, specified as a positive integer.
Position	Position of actor, specified as a real-valued vector of the form $[x\ y\ z]$. Units are in meters.
Velocity	Velocity (v) of actor in the x- y-, and z-directions, specified as a real-valued vector of the form $[v_x\ v_y\ v_z]$. Units are in meters per second.
Roll	Roll angle of actor, specified as a real-valued scalar. Units are in degrees.
Pitch	Pitch angle of actor, specified as a real-valued scalar. Units are in degrees.
Yaw	Yaw angle of actor, specified as a real-valued scalar. Units are in degrees.
AngularVelocity	Angular velocity (ω) of actor in the x-, y-, and z-directions, specified as a real-valued vector of the form $[\omega_x\ \omega_y\ \omega_z]$. Units are in degrees per second.

Figure 23: The ego poses in different scenario fields

4.2. The Actor Vehicles

Actor vehicles are vehicles which are assigned on the road with different position and velocity scenarios in which the ego vehicle's relative motion is tested. In this particular study, there are six actor vehicles assigned on the road.

The actor poses in different fields is imported from Navigation toolbox of MATLAB as shown in figure 23.

Actor poses in vehicle coordinates, specified as a Simulink bus containing a MATLAB structure.

The structure must contain these fields.

Field	Description	Type
`NumActors`	Number of actors	Nonnegative integer
`Time`	Current simulation time	Real-valued scalar
`Actors`	Actor poses	`NumActors`-length array of actor pose structures

Each actor pose structure in `Actors` must contain these fields.

Field	Description
`ActorID`	Scenario-defined actor identifier, specified as a positive integer.
`Position`	Position of actor, specified as a real-valued vector of the form $[x\ y\ z]$. Units are in meters.
`Velocity`	Velocity (v) of actor in the x- y-, and z-directions, specified as a real-valued vector of the form $[v_x\ v_y\ v_z]$. Units are in meters per second.
`Roll`	Roll angle of actor, specified as a real-valued scalar. Units are in degrees.
`Pitch`	Pitch angle of actor, specified as a real-valued scalar. Units are in degrees.
`Yaw`	Yaw angle of actor, specified as a real-valued scalar. Units are in degrees.
`AngularVelocity`	Angular velocity (ω) of actor in the x-, y-, and z-directions, specified as a real-valued vector of the form $[\omega_x\ \omega_y\ \omega_z]$. Units are in degrees per second.

Figure 24: The actor poses in different scenario fields

4.3. The Sensor Fusion

There are basically three types of sensors deployed on the ego vehicle.

The camera is the most important as it is used to track lanes and calibrating multiple actor vehicles in the surrounding.

Radar involves detecting the relative velocity of vehicles in order to predict the collision and decide whether to change the lane.

LiDAR is used for implementing Adaptive Cruise Control (ACC) to maintain the velocity's speed when lane changing is not necessary.

The integral sensors are imported from MATLAB's Sensor Fusion Toolbox to perform detection of the surrounding and environment.

The sensor simulation block on Simulink is represented on Figure 25.

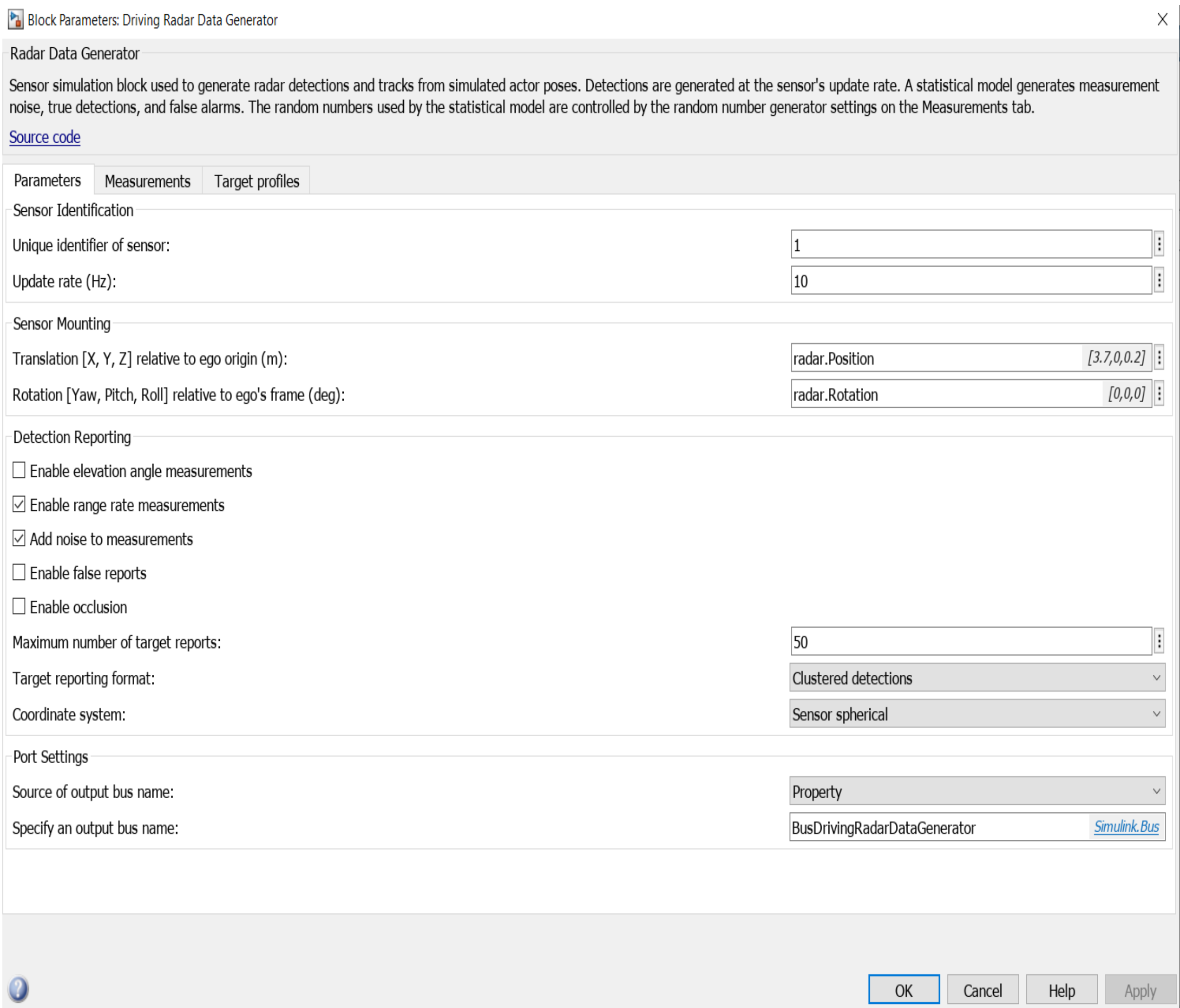

Figure 25: Sensor Simulation Block

4.4. The Simulation Model of Intelligent Decision-Making Algorithm

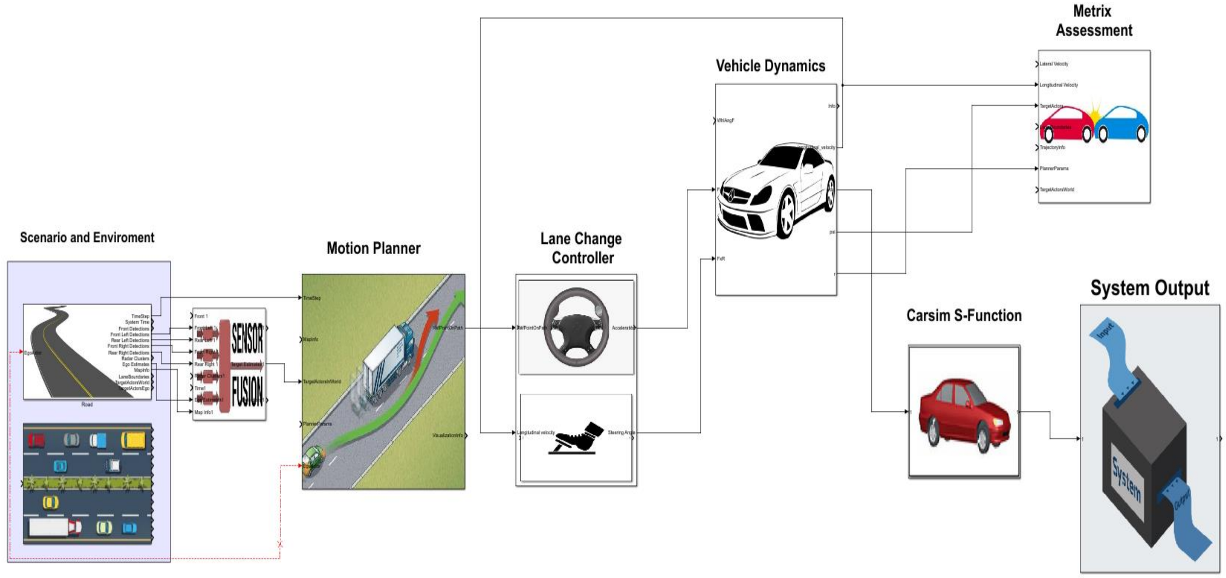

Figure 26: The simulation block diagram of Intelligent Decision-Making Algorithm.

The simulation model is comprised of 6 sub-systems: Scenario and environment; Sensor Fusion, Motion Planner, Lane Change Controller, Vehicle Dynamics and Metrix Assessment.

4.4.1. The Scenario and Environment

This sub-system includes the actor vehicles and road conditions in different scenarios. There are 6 assigned actor vehicles which encounter the ego vehicle. The surrounding environment is imported from Navigation Toolbox of MATLAB.

4.4.2. The Motion Planner

This sub-system is where the trajectory generation and path tracking take place. The desired trajectory generation is performed as per the calculation performed on the previous chapter.

4.4.3. The Lane Change Controller

This sub-system enables the vehicle to perform the appropriate input command to the vehicle through the controllers such as: Steering, Brake, and Throttle. It is integrated with the Automated Driving Toolbox of MATLAB to generate optimized output.

4.4.4. The Vehicle Dynamics

The Bicycle-Model is used which is modeled mathematically in the previous chapter is linked to this subsystem. Therefore, it will store the information of the selected model of the vehicle which can be served as an input for the Metrix assessment.

4.4.5. The Metrix Assessment

This integrates the longitudinal velocity, yaw rate, lateral acceleration, and steering angle with respect to the time gap to command the appropriate decision.

CHAPTER FIVE

RESULTS AND DISCUSSION

5.1. Simulation Results

5.1.1. The Lateral and Longitudinal Velocity

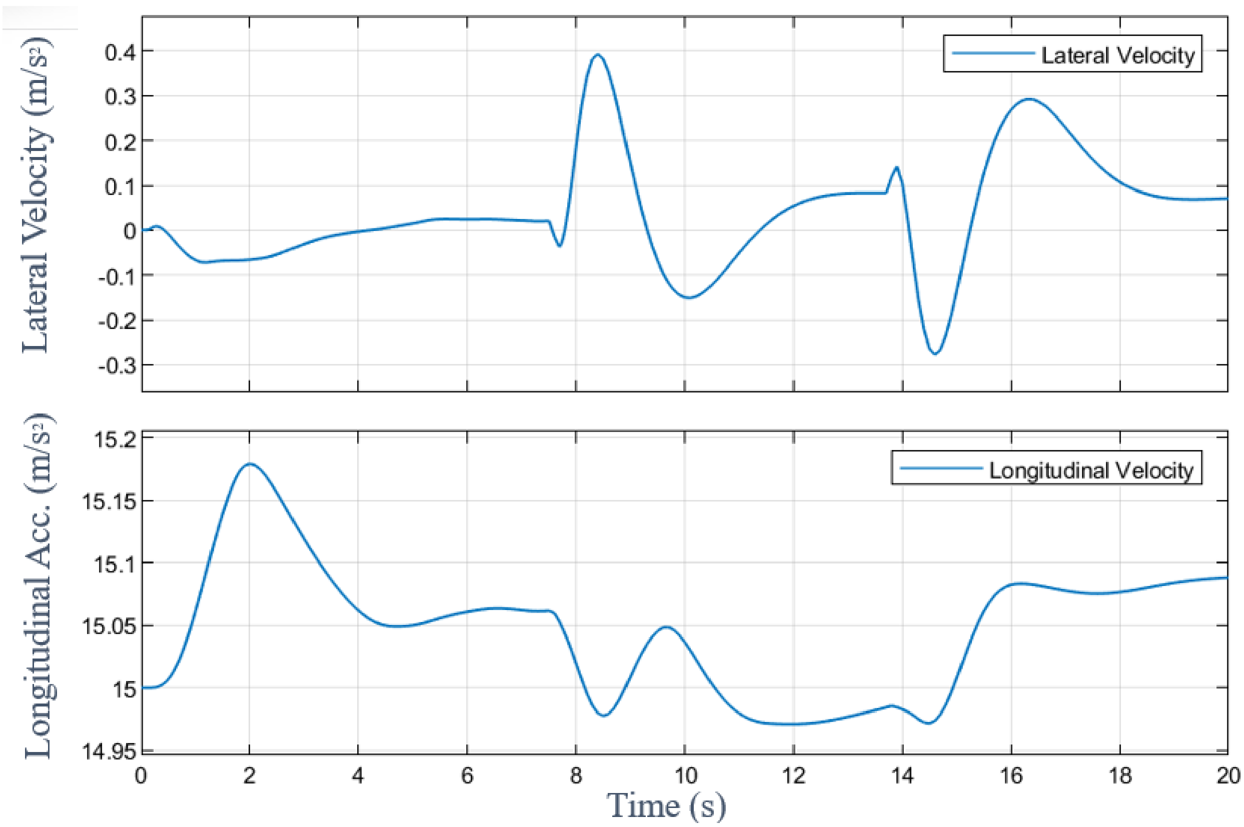

Figure 27: The lateral and Longitudinal Velocity with respect to time.

5.1.2. The Lateral and Longitudinal Acceleration

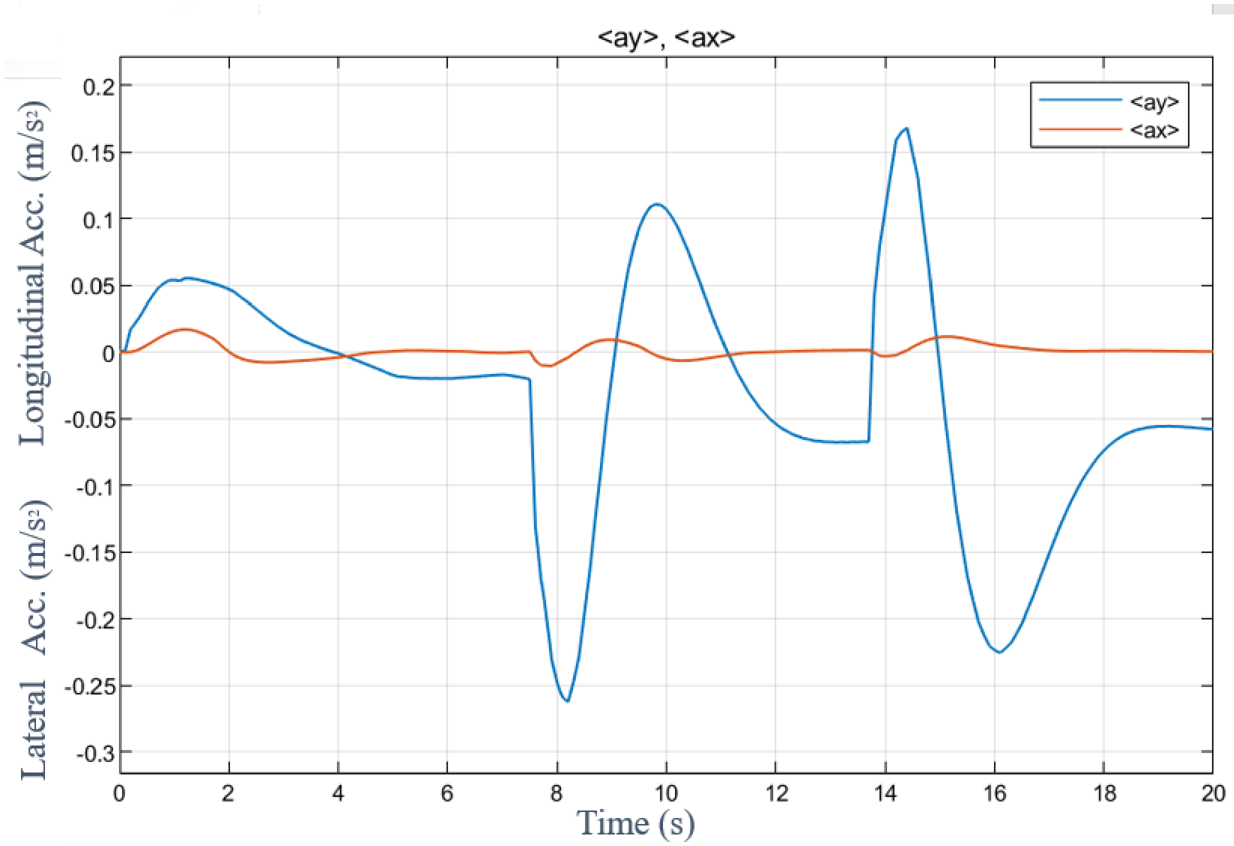

Figure 28: The lateral (blue) and Longitudinal Acceleration(red) with respect to time

5.1.3. The Lateral and Longitudinal Position

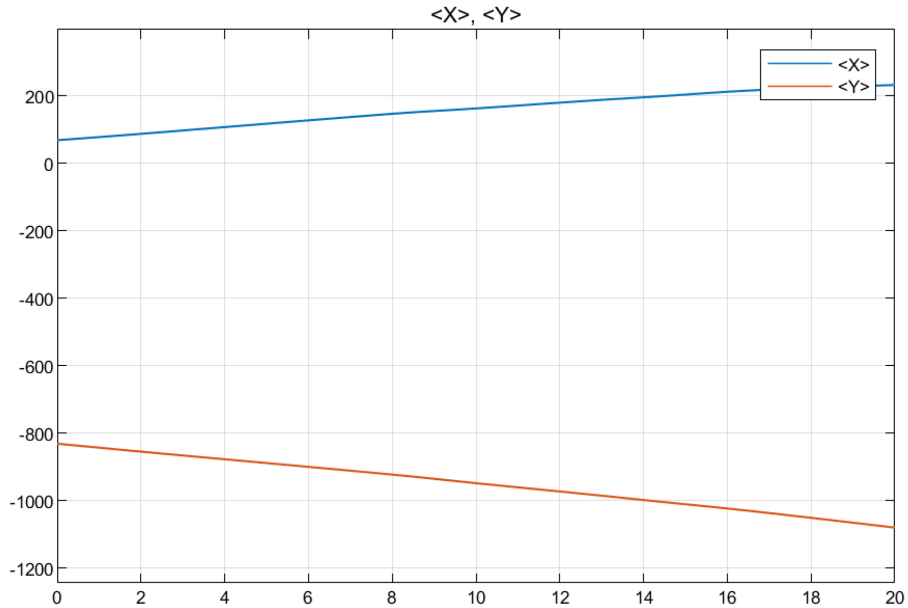

Time(s)

Figure 29: The lateral (red) and Longitudinal Position (blue) (The Global Coordinates) with respect to time in meters.

5.1.4. The Yaw Angle

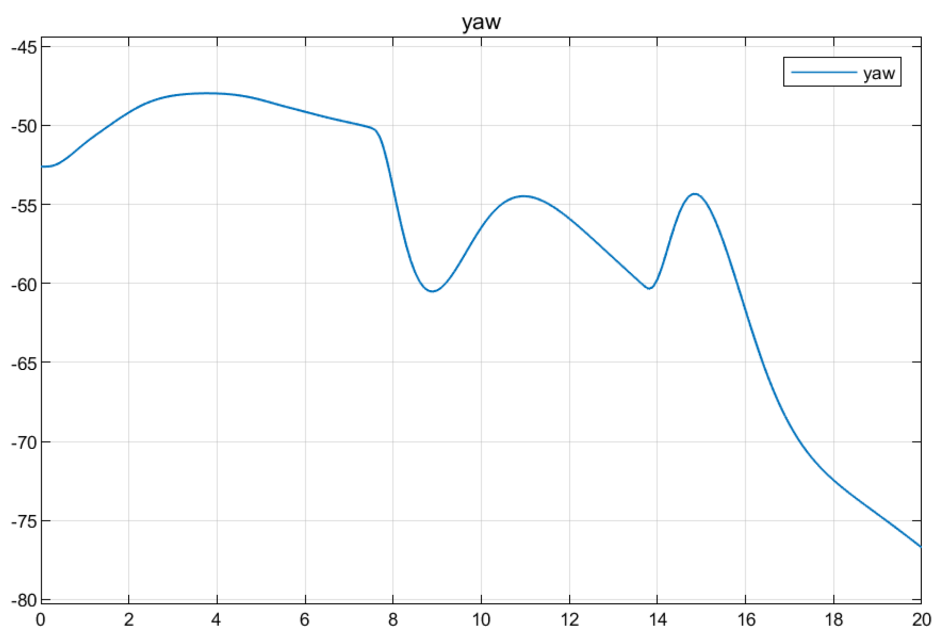

Time(s)

Figure 30: The yaw angle with respect to time

5.1.5. The Yaw Rate

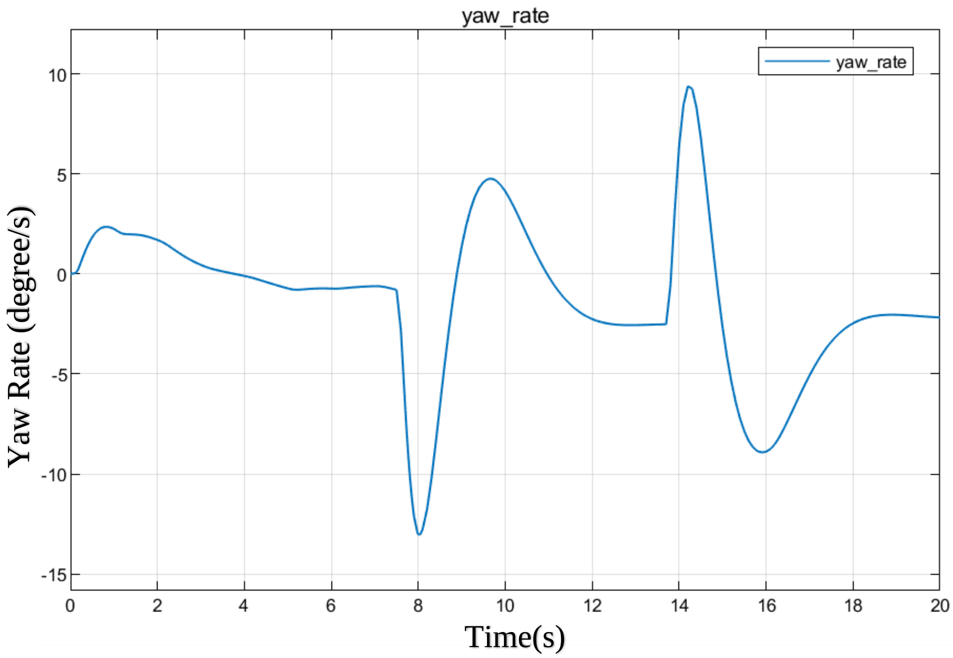

Figure 31: The yaw rate with respect to time

5.1.6. The Steering Angle

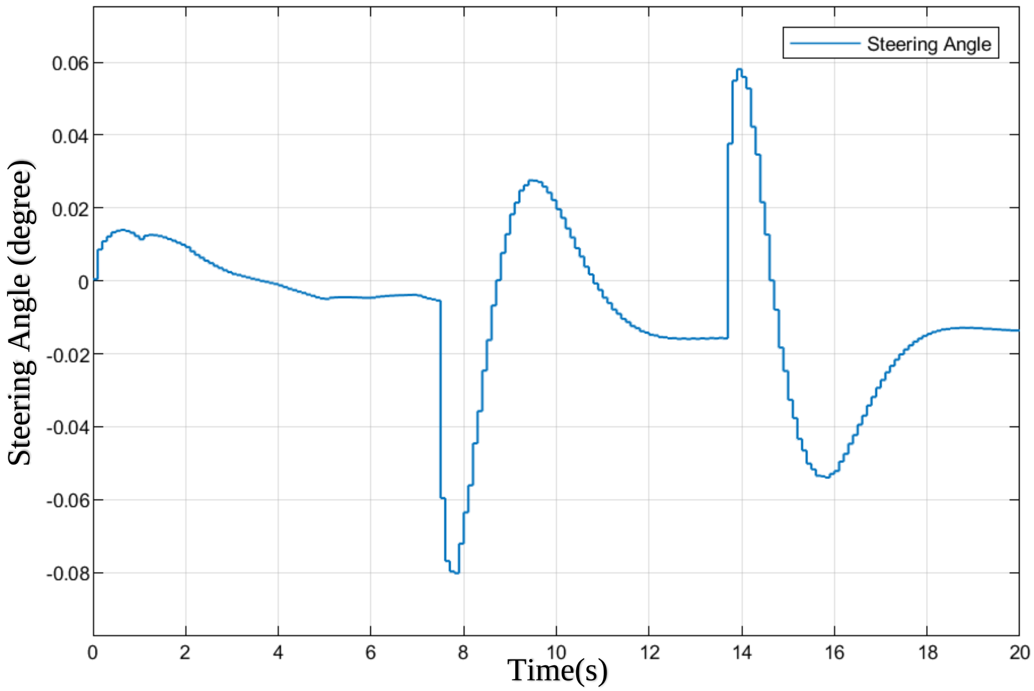

Figure 32: The Steering angle with respect to time

5.1.7. The Steering Angle vs Longitudinal Acceleration

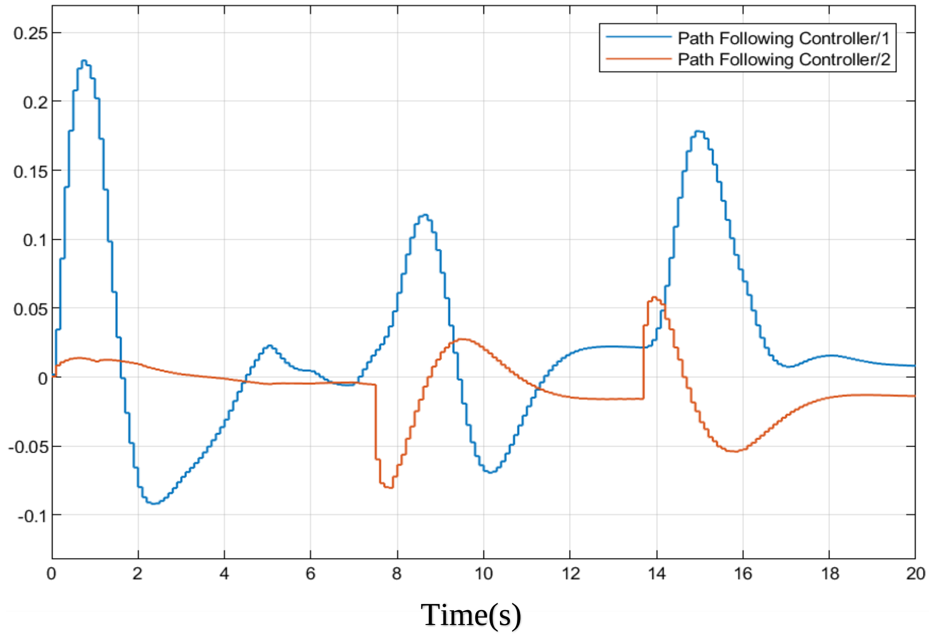

Figure 33: The Steering angle (the red line) Vs Longitudinal Acceleration (the blue line) with respect to time

5.2. Simulation Analysis

The vehicle starts its journey with 15m/s at first. For the first five seconds, the vehicle is maintaining at Cruise Control mode (CC mode) with gradually decreasing of the longitudinal velocity keeping insignificant lateral velocity as shown in figure 28. Since the given initial road structure is curved, the simulation result indicates high initial yaw angle with gradually decreasing flow as shown in figure 31 and 32. The vehicle starts to accelerate that results increase in the longitudinal velocity until it approaches to the preceding vehicles as figure 29 depicts. As it approaches to the actor vehicles, collision is predicted therefore the system switches into Lane Changing mode (LC mode) for the rest of five seconds. As the simulation result indicates, the vehicle will perform high variation of lateral and longitudinal velocity(figure 29). Meanwhile, the vehicle also performs high fluctuation of yaw angle, steering angle and yaw rate until it maintained a stable position between 5^{th}-10^{th} seconds 14^{th} to 16^{th} seconds (Figure 31 and 32). Generally, the vehicle performs lane changes twice.

As a result, the intelligent decision-making algorithm performed the desired output to maintain safe lane change. The simulation results obtained indicates the vehicle performed the desired lane change keeping its safe mode when encountered to different scenarios.

5.3. Visualizing The System Behavior

Running the system model visualizes the system's behavior during a lane shift. Plotting the ego vehicle, tracks, sampling trajectories, capsule list, and other vehicles in the scenario, the Visualization block in the model generates a MATLAB figure that displays the chase view and top view of the scenario as shown in figure 35.

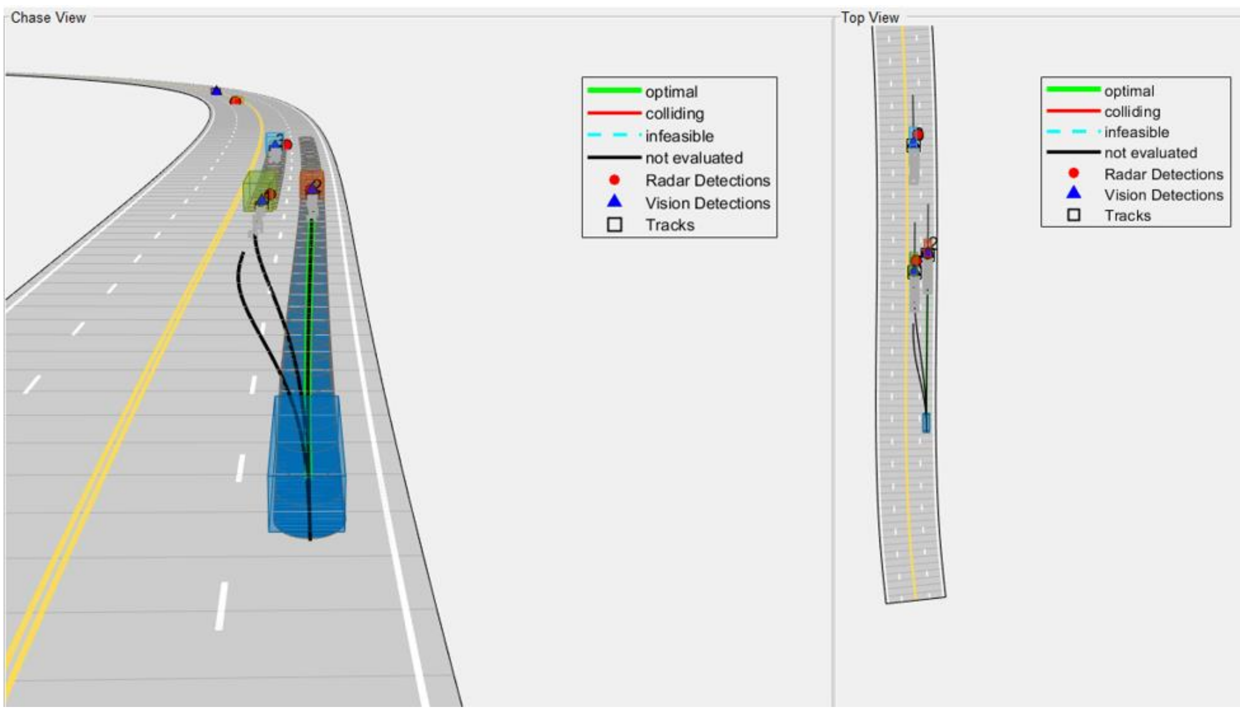

Figure 34: The chase view and top view of the scenario of initial condition

The vehicle was initially travelling in a straight line behind the actor vehicle 2 (the red 1) as shown in figure 35. Then, as it approached closer it has predicted a potential collision with the actor vehicle 2 and detected a safe lane which as it is trajected in a green line (figure 36).

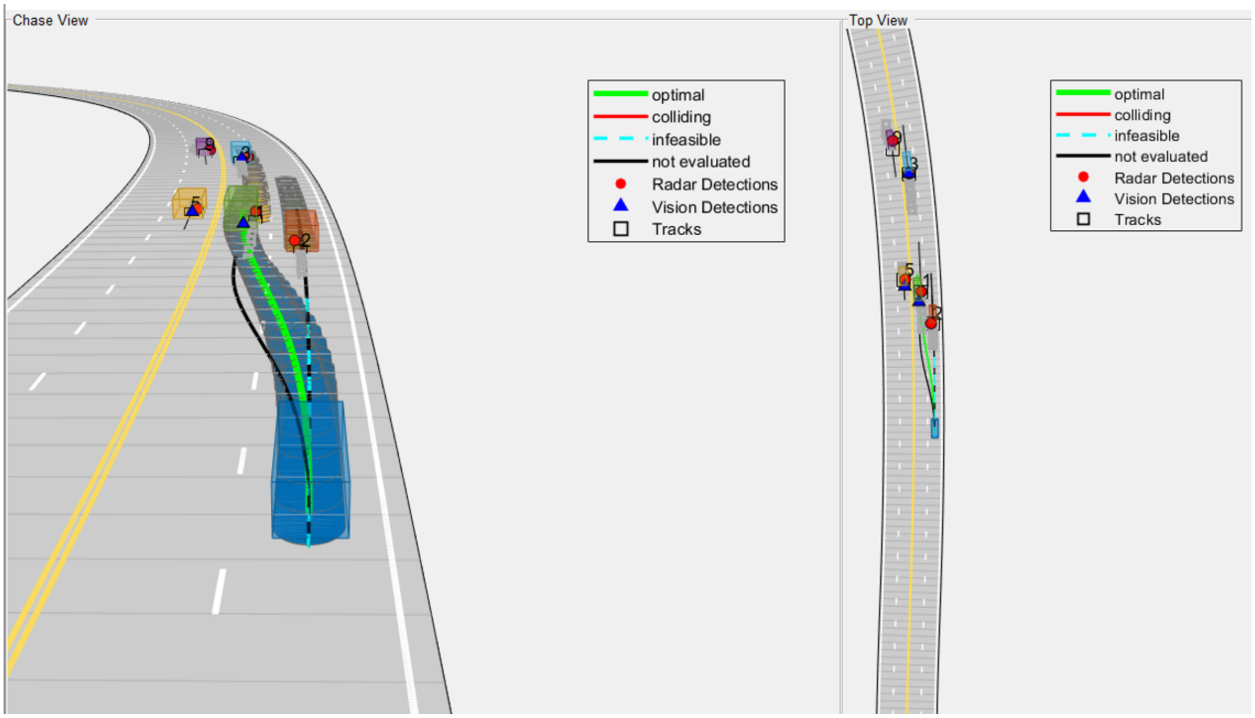

Figure 35: Detection of appropriate lane to decide a lane change

The ego vehicle automatically makes a lane shift to the left (Figure 37) and to the right in the same manner (Figure 39) as an emergency maneuvering.

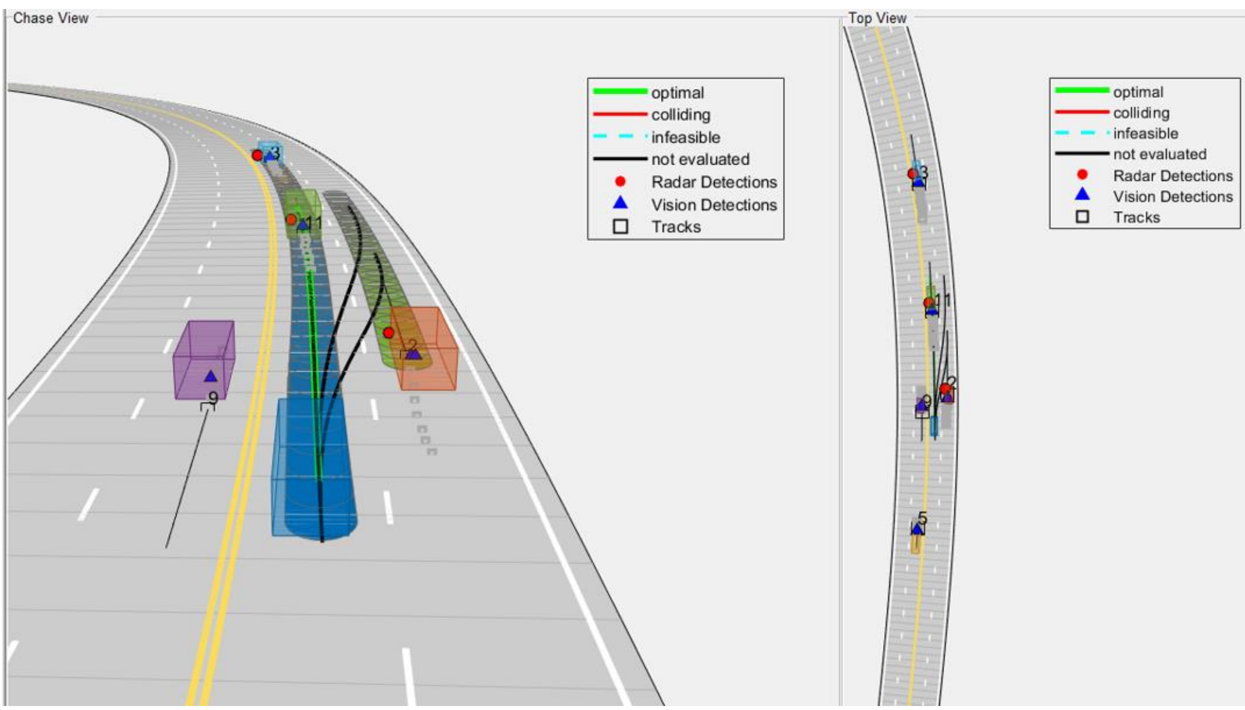

Figure 36: Automatic shift to the left

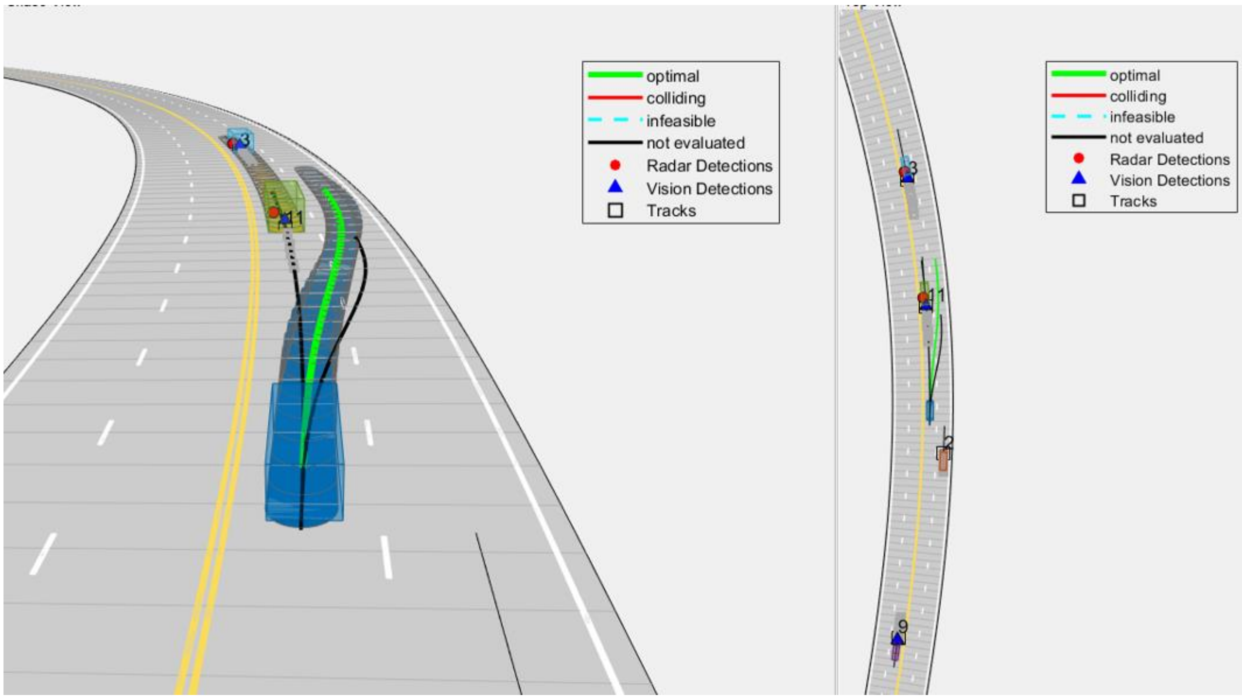

Figure 37: Detection of potential safe lane change to the right

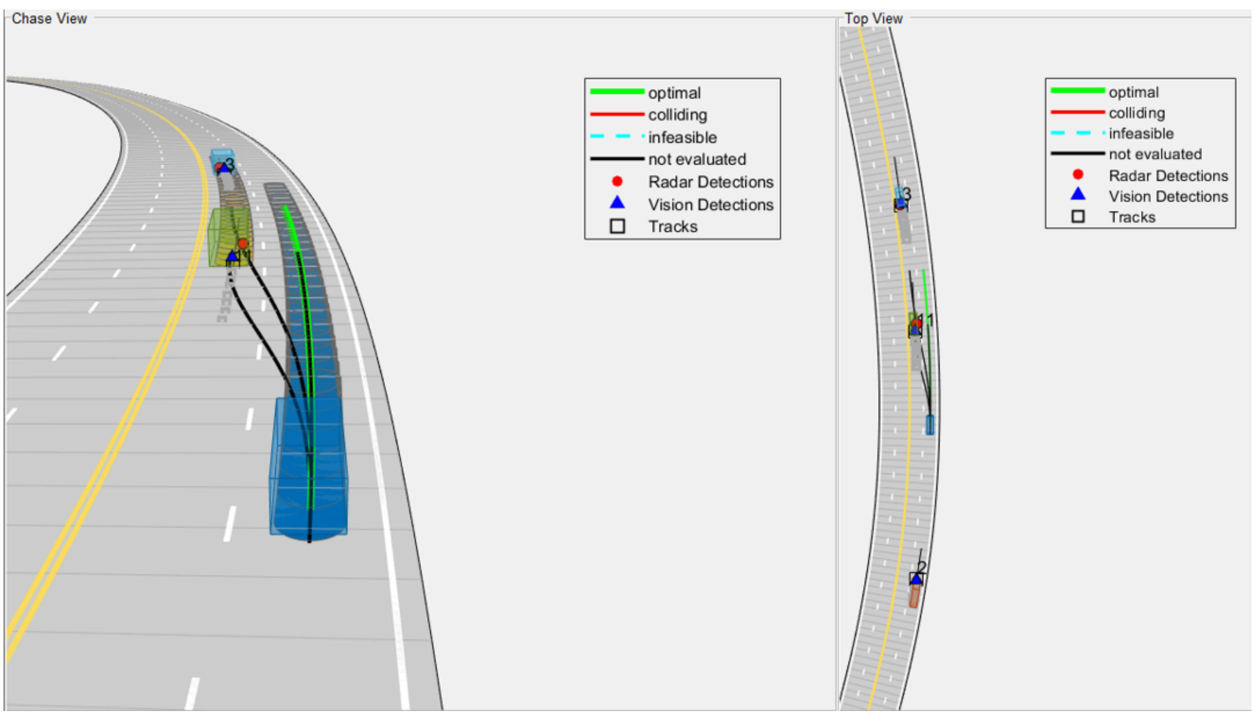

Figure 38: The final lane shift to the right

CONCLUSION AND RECOMMENDATION

- The functioning of the system can be further improved in a number of areas thanks to the work in this thesis. A straight, even road with a straight-line driving condition was among the initial assumptions used prior to modeling. For real-world driving, new variables for curving and uneven roadways can be included. The idea of vehicle-to-vehicle communication can be applied to the model thanks to the rapid advancement of technology. By doing so, the model's size will be decreased and unnecessary functionality will be replaced. The usage of the current sensors is another area where the research might be expanded. To help the system make better decisions, sensor measurements like a steering angle, speed, and lateral position can be transformed into continuous places and transitions. This will enhance the simulations by introducing more intricate scenarios.
- The intelligent decision-making algorithm is validated as it has generated precise output as it passes the given environmental scenario and road condition. It thesis found to be valuable contribution in optimization of decision-making in lane changing condition specifically. It can be applied by combining with electronic stability control (ESC), anti-lock brake system (ABS) and other general collision avoidance systems.
- A control strategy can be used in regard to enhancing the model itself. Conflicts between several enabled transitions are intended to be resolved by this. Additionally, it can include adding decision transitions to the current model or a new Petri net controller. The model can also be transformed into probabilistic or timed hybrid Petri nets. These kinds would take event probabilities and timed transition firing into account. These recommendations are aimed at system optimization in addition to enhancing functionality.

- This thesis motivates to further studies of vehicles safety with lane-changing cooperating with the advancement of Electronic Stability Control (ESC), Active Toque Distribution and Passenger Comfort and more. The technology advancement is bringing vehicles with high speed and acceleration variation; the safety advancement in vehicle model for stability and balance is enormously helpful. As a result, a lot work and inspiring future works are indicated and look forwarded.

REFERENCES

Aksun Güvenç, B., & Kural, E. (2006). *Adaptive cruise control simulator: a low-cost, multiple-driver-in-the-loop simulator, Control System Magazine, vol. 26, pp. 42-5*.

Ararat, Ö., & Güvenç, B. A. (n.d.). *A Survey of Recent Developments in Collision Avoidance , Collision Warning and Inter-Vehicle Communication Systems*. 238–246.

Bakker, E., Nyborg, L., & Pacejka, H. B. (1987). Tyre Modelling for Use in Vehicle Dynamics Studies. In *Transactions* (Vol. 96). https://www.jstor.org/stable/44470677

Bascunana, J. L., & Mesa, C. (1997). *Analysis of Lane Change Crash Avoidance Reprinted from: Systems and Issues in ITS (SP-1106) Future Transportation Technology Conference and Exposition*.

Burgett Arthur Carter, A., & Preziotti, G. (n.d.). *AN ALGORITHM FOR REAR-END COLLISION AVOIDANCE WARNING SYSTEMS*.

Carroll, K. P., McClaran, S. R., Nelson, E. L., Barnett, D. M., Friesen, D. K., & Williams, G. N. (1992). AUV path planning: An A∗ approach to path planning with consideration of variable vehicle speeds and multiple, overlapping, time-dependent exclusion zones. *Proceedings of the 1992 Symposium on Autonomous Underwater Vehicle Technology*, *AUV 1992*, 79–84. https://doi.org/10.1109/AUV.1992.225191

Chae, H., & Yi, K. (2020). Virtual Target-Based Overtaking Decision, Motion Planning, and Control of Autonomous Vehicles. *IEEE Access*, *8*, 51363–51376. https://doi.org/10.1109/ACCESS.2020.2980391

Chiang, H. H., Chen, Y. L., Wu, B. F., & Lee, T. T. (2014). Embedded driver-assistance system using multiple sensors for safe overtaking maneuver. *IEEE Systems Journal*, *8*(3), 681–698. https://doi.org/10.1109/JSYST.2012.2212636

Dai, M., Wang, J., Yin, G., & Chen, N. (2017). *Dynamic Output-feedback Robust Control for Vehicle Path Tracking Considering Different Human Drivers' Characteristics*.

Do, Q. H., Tehrani, H., Mita, S., Egawa, M., Muto, K., & Yoneda, K. (2017). Human drivers based active-passive model for automated lane change. *IEEE Intelligent Transportation Systems Magazine*, *9*(1), 42–56. https://doi.org/10.1109/MITS.2016.2613913

Doi, A., Butsuen, T., Niibe, T., Takagi, T., Yamamoto, Y., & Seni, H. (1994). Development of a rear-end collision avoidance system with automatic brake control. In *JSAE Review* (Vol. 15).

Falcone, P., Borrelli, F., Asgari, J., Tseng, H. E., & Hrovat, D. (2007). Predictive active steering control for autonomous vehicle systems. *IEEE Transactions on Control Systems Technology*, *15*(3), 566–580. https://doi.org/10.1109/TCST.2007.894653

Fujita, Y., Akuzawa, K., & Sato. (1995). Radar Brake System, Annual Meeting of ITS America. *Radar Brake System, Annual Meeting of ITS America*.

Godbole, D. N., Hagenmeyer, V., Sengupta, R., & Swaroopl, D. (1997). *Design of Emergency Maneuvers for Automated Highway System: Obstacle Avoidance Problem* (Vol. 4).

González, C., Llorca, D. F., Villagra, J., Pérez, J., Sotelo, M. A., & Parra, I. (1999). *Vicente Milanés*.

Hang, P., & Chen, X. (2021). Path tracking control of 4-wheel-steering autonomous ground vehicles based on linear parameter-varying system with experimental verification. *Proceedings of the Institution of Mechanical Engineers. Part I: Journal of Systems and Control Engineering*, *235*(3), 411–423. https://doi.org/10.1177/0959651820934572

Hang, P., Chen, X., Zhang, B., & Tang, T. (2018). Longitudinal Velocity Tracking Control of a 4WID Electric Vehicle. *IFAC-PapersOnLine*, *51*(31), 790–795. https://doi.org/10.1016/j.ifacol.2018.10.129

Hegeman, G., Brookhuis, K., & Hoogendoorn, S. (2005). Opportunities of advanced driver assistance systems towards overtaking. *European Journal of Transport and Infrastructure Research(EJTIR)*, *5*(4), 281–296.

J. D. Chovan et al. (1994). *Examination of Lane Change Crashes and Potential IVHS Countermeasures DOT HS 808 071 Final Report*.

J.-S.Wang, & R. R. Knipling. (1994). *Lane Change/Merge Crashes: Problem Size Assessment and Statistical Description*.

Karunakaran, D., Berrio, J. S., Worrall, S., & Nebot, E. (2022). *Parameterisation of lane-change scenarios from real-world data*. 2607–2613. https://doi.org/10.1109/itsc55140.2022.9921981

Li, C., Wang, J., Wang, X., & Zhang, Y. (2016). A model based path planning algorithm for self-driving cars in dynamic environment. *Proceedings - 2015 Chinese Automation Congress, CAC 2015, September 2020*, 1123–1128. https://doi.org/10.1109/CAC.2015.7382666

Li, K., & Ioannou, P. (2004). Modeling of traffic flow of automated vehicles. *IEEE Transactions on Intelligent Transportation Systems*, *5*(2), 99–113. https://doi.org/10.1109/TITS.2004.828170

Li, M., Wang, H., Wang, Z., Jiang, Y., Ye, M., Chen, K., & Zhang, H. (2019). Anti-collision system design of vehicle lane change overtaking. *Proceedings - 2019 4th International Conference on Mechanical, Control and Computer Engineering, ICMCCE 2019*, 571–577. https://doi.org/10.1109/ICMCCE48743.2019.00132

Lin, Y. C., Lin, C. L., Huang, S. T., & Kuo, C. H. (2021). Implementation of an autonomous overtaking system based on time to lane crossing estimation and model predictive control. *Electronics (Switzerland)*, *10*(18). https://doi.org/10.3390/electronics10182293

Macadam, C. C. (2003). Understanding and Modeling the Human Driver. In *Swets & Zeitlinger* (Vol. 40).

Malayjerdi, E., Sell, R., Malayjerdi, M., Udal, A., & Bellone, M. (2022). Practical path planning techniques in overtaking for autonomous shuttles. *Journal of Field Robotics*, *39*(4), 410–425. https://doi.org/10.1002/rob.22057

Seiler, P., Song, B., & Hedrick, J. K. (1998). *Development of a Collision Avoidance System*.

Suh, J., Chae, H., & Yi, K. (2018). Stochastic Model-Predictive Control for Lane Change Decision of Automated Driving Vehicles. *IEEE Transactions on Vehicular Technology*, *67*(6), 4771–4782. https://doi.org/10.1109/TVT.2018.2804891

Wang, J., Wang, J., Wang, R., & Hu, C. (2017). A framework of vehicle trajectory replanning in lane exchanging with considerations of driver characteristics. In *IEEE Transactions on Vehicular Technology* (Vol. 66, Issue 5, pp. 3583–3596). Institute of Electrical and Electronics Engineers Inc. https://doi.org/10.1109/TVT.2016.2609154

Z. Shiller, & S. Sunder. (1998). *Emergency lane-change maneuvers of autonomous vehicles*.

Zhang, K., Wang, J., Chen, N., & Yin, G. (2019). A non-cooperative vehicle-to-vehicle trajectory-planning algorithm with consideration of driver's characteristics. *Proceedings of the Institution of Mechanical Engineers, Part D: Journal of Automobile Engineering*, *233*(10), 2405–2420. https://doi.org/10.1177/0954407018783394

Nomenclatures

C_p	Location of the approaching vehicle	θ	The relative yaw angle of the vehicle (rad)
l_p	Length of the approaching vehicle (m)	v	The velocity of the vehicle (km/hr)
w_p	Width of the approaching vehicle (m)	a_x	Throttle $(\mathrm{m/s^2})$
φ	Distance between the ego and approaching vehicles (cm)	W	Width of the road(m)
α	Lateral coordinate of an edge pixel	N_p	Output horizon
β	Longitude coordinate of an edge pixel	N_c	Control horizon
ρ	Line characterization parameter	R_s	Object
ϕ	The angle between the x-axis and the fitted line of the edge point (rad)	m	State vector of the vehicle
y_u	Lateral distance between the front left tire and the lane line (cm)	u	Control inputs
y_{rr}	Lateral distance between the front right tire and the lane line (cm)	n	Control outputs
y_l	Distance from the vehicle's center of gravity to the left lane line (cm)	T	Sampling interval
y_r	Distance from the vehicle's center of gravity to the right lane line (cm)	k	Control interval
ψ	Relative yaw angle (rad)	κ	Slope of the overtaking constrained area
l_f	Length of the ego vehicle (m)	y_{psafe}	Lateral location of the approaching vehicle-collision avoidance area
q	Width of the ego vehicle (m)	x_{psafe}	Longitudinal location of the approaching vehicle-collision avoidance area
R_{vl}	Radius of the path (m)	O_v	Center of the DLC arc
ξ_{ll}	Angle of the DLC arc (rad)	x	The global longitudinal location the rear wheel
δ_f	Constant steering angle (rad)	y	The global lateral location of the rear wheel